

Université de Montréal

***In situ*-Forming Injectable Organogel Implant for
Sustained Release of Rivastigmine**

par

Anda Vintiloiu

Sciences pharmaceutiques

Faculté de Pharmacie

Mémoire présenté à la Faculté des études supérieures
en vue de l'obtention du grade de Maître en sciences (M.Sc.)

Sciences pharmaceutiques

Option technologie pharmaceutique

Mai 2007

© Anda Vintiloiu, 2007

QV

705

U58

2007

V.009

Direction des bibliothèques

AVIS

L'auteur a autorisé l'Université de Montréal à reproduire et diffuser, en totalité ou en partie, par quelque moyen que ce soit et sur quelque support que ce soit, et exclusivement à des fins non lucratives d'enseignement et de recherche, des copies de ce mémoire ou de cette thèse.

L'auteur et les coauteurs le cas échéant conservent la propriété du droit d'auteur et des droits moraux qui protègent ce document. Ni la thèse ou le mémoire, ni des extraits substantiels de ce document, ne doivent être imprimés ou autrement reproduits sans l'autorisation de l'auteur.

Afin de se conformer à la Loi canadienne sur la protection des renseignements personnels, quelques formulaires secondaires, coordonnées ou signatures intégrées au texte ont pu être enlevés de ce document. Bien que cela ait pu affecter la pagination, il n'y a aucun contenu manquant.

NOTICE

The author of this thesis or dissertation has granted a nonexclusive license allowing Université de Montréal to reproduce and publish the document, in part or in whole, and in any format, solely for noncommercial educational and research purposes.

The author and co-authors if applicable retain copyright ownership and moral rights in this document. Neither the whole thesis or dissertation, nor substantial extracts from it, may be printed or otherwise reproduced without the author's permission.

In compliance with the Canadian Privacy Act some supporting forms, contact information or signatures may have been removed from the document. While this may affect the document page count, it does not represent any loss of content from the document.

Université de Montréal
Faculté des études supérieures

Ce mémoire intitulé :
In situ-Forming Injectable Organogel Implant for Sustained Release of Rivastigmine

présenté par
Anda Vintiloiu

a été évalué par un jury composé des personnes suivantes:
Dr. Françoise Winnik, président-rapporteur
Dr. Jean-Christophe Leroux, directeur de recherche
Dr. Didier Hoarau, membre du jury

Résumé

Les organogels présentent un grand intérêt en pharmacie galénique en raison de leur facilité de préparation ainsi que leur capacité de libérer un principe actif de façon prolongée. Dans le cadre de ce projet, un organogel a été évalué comme implant injectable pour la libération soutenue de la rivastigmine, un inhibiteur de la cholinestérase utilisé pour le traitement de la maladie d'Alzheimer. Le gel a été préparé en dissolvant 5 – 15% (*p/p*) de N-lauroyle L-alanine methyl ester (SAM) dans l'huile de carthame contenant la rivastigmine dissoute ou son sel d'hydrogène tartrate dispersé. Les mesures de températures de transition, obtenues par calorimétrie différentielle à balayage et par spectroscopie infrarouge, ont indiqué un affaiblissement de la structure de l'organogel suite à l'incorporation de drogue dissoute (4% *p/p*). À la même concentration, aucune modification en terme de température de transition n'a été détectée dans les gels contenant le principe actif sous forme sel, indiquant une interférence négligeable avec la matrice gélifiante. Ces mêmes gels ont démontré des profils de libération *in vitro* ayant le plus faible effet « *burst* », avec moins de 15% du principe actif libéré durant la première journée. Des études pharmacocinétiques réalisées avec des rats ayant reçu par la voie sous-cutanée des organogels 10% SAM ont mis en évidence une libération maintenant des concentrations plasmatiques de rivastigmine dans la fenêtre thérapeutique pendant 11 jours. De plus, cette formulation a permis une réduction de la concentration plasmatique maximale d'un facteur de 5 par rapport à la formulation contrôle constituée d'huile sans gélateur. En conclusion, ce projet a démontré la possibilité d'utiliser les organogels de SAM en tant que formulation à libération prolongée pour le traitement de la maladie d'Alzheimer.

Mots clés: organogel, libération prolongée, implant autoformant *in situ*, rivastigmine, maladie d'Alzheimer.

Abstract

Organogels are interesting systems holding great promise for drug delivery applications owing to their ease of preparation and potential for long-term release. This project investigated the use of such an organogel as an injectable implant for the sustained release of rivastigmine, a cholinesterase inhibitor used in the treatment of Alzheimer's disease. Such a formulation is expected to provide a simplified dosing schedule and potentially reduce side effects associated to plasma peak concentrations. The gel was prepared by dissolving 5 - 15% (w/w) N-stearoyl L-alanine methyl ester (SAM) in safflower oil containing either dissolved rivastigmine or its dispersed hydrogen tartrate salt. Differential scanning calorimetry and infrared spectroscopy indicated a weakening of the oleogel structure by the incorporation of dissolved drug (4% w/w), as proven by decreasing gel-sol transition temperatures. At the same concentration, no such changes were detected for gels containing the dispersed drug salt, indicating negligible interference of the latter with gel auto-assembly. *In vitro* release profiles of gels containing dispersed rivastigmine showed the lowest burst (<15% in the first day). A pharmacokinetic study, in which rats were injected subcutaneously with 10% SAM gels containing the dispersed drug, demonstrated a sustained rivastigmine release within therapeutic range for up to 11 days. Peak plasma levels were found to be well below the toxic threshold and up to five times lower than for the control oil formulation. Overall this project established SAM gels to be a promising option for a sustained-release formulation in the treatment of Alzheimer's disease.

Keywords: organogel, sustained release, *in situ*-forming implant, rivastigmine, Alzheimer's disease.

Table of contents

Résumé	iv
Abstract	vi
List of tables	x
List of figures	xi
List of abbreviations	xvi
Acknowledgements	xviii
CHAPTER 1: ALZHEIMER'S DISEASE	
1. Introduction	2
2. Pathophysiology	2
3. Treatment options	4
3.1. Cholinesterase inhibitors	4
3.2. Other therapies	6
References	8
CHAPTER 2:	
SUSTAINED RELEASE FORMULATIONS	9
References	15
CHAPTER 3:	
ORGANOGELES AND THEIR USE IN DRUG DELIVERY – A REVIEW	
1. Abstract	18
2. Introduction	19
3. Organogel properties	22
3.1. Low molecular weight gelators	22
3.1.1. Solid-matrix organogels	23
3.1.1.1. <i>General gelation considerations</i>	23
3.1.1.2. <i>Chirality effects</i>	28
3.1.2. Fluid-matrix organogels	31

3.1.2.1. <i>Lecithin organogels</i>	31
3.1.2.2. <i>Fatty-acid derived-sorbitan organogels</i>	35
3.2. Polymeric gelators	36
4. Organogels in drug delivery	38
4.1. Dermal and transdermal formulations	40
4.1.1. Lecithin organogels	41
4.1.2. Fatty-acid derived-sorbitan organogels	43
4.1.3. Organogels based on other low molecular weight gelators	43
4.1.4. Poly(ethylene) organogels	44
4.2. Parenteral depot formulations	44
4.3. Trans-mucosal and oral formulations	47
5. Summary and conclusions	50
6. Acknowledgements	51
References	52
CHAPTER 4: ARTICLE	57
1. Abstract	58
2. Introduction	69
3. Materials and methods	61
3.1. Materials	61
3.2. Preparation of implants	62
3.2.1. Dispersed-RHT gels	62
3.2.2. Dissolved-RB gels	62
3.3. Characterization	63
3.3.1. Rheology	63
3.3.2. Differential scanning calorimetry (DSC)	63
3.3.3. Thermal Fourier-transform infrared spectroscopy (FTIR)	64
3.3.4. Microscopy	65
3.4. <i>In vitro</i> release of rivastigmine	65
3.4.1. Release study	65
3.4.2. HPLC method	66

3.5. Pharmacokinetic study	67
3.6. Statistical analysis	68
4. Results and discussion	69
4.1. Physicochemical characterization of oleogel	69
4.1.1. Rheology	69
4.1.2. DSC	71
4.1.3. FTIR	73
4.1.4. Microscopy	75
4.1.5. <i>In vitro</i> release	77
4.1.6. Pharmacokinetic study	79
5. Conclusion	83
6. Acknowledgements	83
References	84
CHAPTER 5: RESULTS AND DISCUSSION	86
CHAPTER 6: CONCLUSION AND OUTLOOK	94
APPENDIX : METHODOLOGY	97

List of tables

CHAPTER 1

Table I: Current drugs on the market or in clinical trials for the treatment of AD.

5

CHAPTER 3

Table I: Organogel formulations used in drug delivery

39

CHAPTER 4

Table 1. Gel characterization: 10% (w/w) SAM oleogels containing various concentrations of rivastigmine incorporated by dissolution or dispersion were characterized by rheological analysis, DSC and IR (mean \pm SD).

72

Table II: Pharmacokinetic parameters of the different formulations injected to rats (n=6)

80

List of figures

CHAPTER 1

Figure 1: The hypothesis of the amyloid cascade proposes a progression from the generation of β -amyloid precursor protein (APP), through multiple secondary steps, to cell death.

3

CHAPTER 3

Figure 1: Organogel classification.

20

Figure 2: Solid-matrix (strong) *versus* fluid-matrix (weak) organogels. A) Solid-matrix gels are more robust due to their permanent solid-like networks in which the junction points are relatively large (pseudo)crystalline microdomains (circled area). B) Fluid-matrix gels have transient networks in which junction points are most often simple chain entanglements. Additional kinetic features such as dynamic exchange of gelator molecules with the bulk liquid as well as chain breaking/recombination (arrows) may occur.

22

Figure 3: A) Photograph depicting the opaque N-stearoyl-L-alanine methyl ester organogel; B) optical micrograph showing the fibrous aggregates responsible for gelation; C) molecular packing within fibers.

25

Figure 4: A) optical micrograph of a (4%) hexatriacontane (C36) organogel in octanol viewed through crossed polars; B) a cartoon representation of the microplatelets

observed in A); C) depiction of the lamellar orthorhombic molecular packing inside the platelets, showing the directions of microplatelet growth.

25

Figure 5: A) Transmission electron micrograph of organogel of a crown ether phthalocyanine in chloroform, showing a left-handed coil. B) Schematic representation of helical fibers in A). C) The helical aggregates are formed by the stacking of crown ether rings with a staggering angle, constant in magnitude and direction. D) Supercoiled structure is obtained from side-on aggregation of individual fibers.

29

Figure 6: A) Gelator chirality effect showing a decrease in DSC-determined sol-gel (white bars) and gel-sol (solid bars) transitions in racemic organogels (N-stearoyl D/L-alanine methyl ester, D/L-SAM) with respect to enantiomerically-pure L- and D-SAM organogels, respectively (mean, $n = 2$). B) FTIR analysis showing the proportion of free gelator amide bonds in gel systems, as determined from the band intensity ratio of amide I peaks at 1685 and 1648 cm^{-1} (I_{1685}/I_{1648}), as a function of temperature. Enantiomerically pure L-SAM (■) organogels showed higher gel-sol transition temperatures than D/L-SAM (□) organogels (mean \pm SD, $n = 3$).

30

Figure 7: Formation of a three-dimensional network of reverse cylindrical micelles in lecithin organogel, involving hydrogen bonding between lecithin and polar solvent molecules.

32

Figure 8: Plot of zero shear viscosity *versus* the water-to-lecithin molecular ratio (w_0). Dotted lines roughly indicate boundaries between various phase regions.

34

Figure 9: A) Plasma concentrations of leuprolide after the subcutaneous administration of a control w/o emulsion (squares) and various organogel formulations (circles and triangles; SAM and SAE: N-stearoyl methyl or ethyl ester, respectively). B) Plasma concentrations of testosterone after the administration of the formulations in a). The dotted line represents the chemical castration threshold (mean \pm SEM, n=5-6).

48

CHAPTER 4

Figure 1: Molecular structures of a) rivastigmine base and b) N-stearoyl L-alanine methyl ester (SAM).

61

Figure 2: Rheology experiments of 10% w/w SAM oleogel in safflower oil containing no drug (■,□), 4% w/w dissolved RB (●,○), and 5% dispersed RHT (▲,△). Full and empty symbols correspond to G' and G'', respectively. a) Strain sweep at constant frequency (1 Hz) and temperature (25°C); b) Frequency sweep at constant strain (0.01%) and temperature (25°C); c) Determination of the T_{GS} (■,□) at constant strain (0.005 %) and frequency (1 Hz).

69

Figure 3: DSC analyses showing gel-sol transitions for drug-free gels (□), for gels containing 5% (w/w) dispersed RHT (■), and for gels containing RB dissolved at 4 (Δ), 20 (○), and 40% (w/w) (◇). Curves are offset on the y-axis for improved clarity. ΔH and T_{GS} values were calculated from the area under the curve and the temperature corresponding to the peak transition, respectively.

71

Figure 4: Thermal evolution, as probed by FTIR spectroscopy. The intensity ratio of the amide I peak components (I₁₆₈₅/I₁₆₄₈) was monitored as an indication of H-bond

disruption between SAM molecules during gel heating from 20 to 75 °C. Arrows indicate changes from the gel (low temperatures) to the liquid (high temperatures) state.

73

Figure 5: FTIR analysis showing the proportion of free amide bonds in drug-loaded gels, as determined from the band intensity ratio of amide I peaks at 1685 and 1648 cm^{-1} (I_{1685}/I_{1648}), as a function of temperature for gels containing dissolved RB at different concentrations: 0 (\square), 4 (Δ) and 40% (w/w) (\circ) (Mean \pm SD, $n = 3$).

74

Figure 6: a) An inverted tube containing 10% (w/w) SAM gel is shown at room temperature to demonstrate the cohesiveness of the system. The inset shows an optical microscopy image of the oleogel network. ESEM images of a 10% (w/w) SAM b) drug-free oleogel and c) oleogel containing dissolved-RB (5% w/w). Finally, an ESEM image is shown of d) a dried formulation, obtained after complete solvent evaporation from an organogel of 10% SAM in toluene.

76

Figure 7: *In vitro* release experiments for formulations varying in SAM and NMP content as well as in drug incorporation method (dissolution *vs.* dispersion). A control RHT solution in PBS (X) was tested. Release experiments from formulations containing dissolved RB are represented by solid symbols: oil formulation (\bullet), 10% SAM gel with (\blacksquare) and without NMP (\blacktriangle); release experiments from gels containing dispersed RHT are represented by hollow symbols: oil formulation (\circ) and 10% SAM gel with (\square) and without NMP (Δ) (Mean \pm SD, $n = 3$).

78

Figure 8: Blood concentration of rivastigmine after the s.c. administration of a 10 mg/kg dose of saline RHT solution (\blacktriangle), and 18 mg/kg doses of RHT dispersed in oil (\blacksquare), in 5% (\triangle), and in 10% (*w/w*) SAM gel (\square). (Mean \pm SEM, $n = 6$) SEM rather than SD values were used for the error bars in order to reduce clutter and improve the clarity.

80

CHAPTER 5

Figure 1: Average hardness of oleogels varying in SAM concentration, obtained by texture profile analysis (Mean \pm SD, $n = 3$).

88

Figure 2: Gelator chirality effect showing a decrease in DSC-determined sol-gel (white bars) and gel-sol (solid bars) transitions in racemic organogels (D/L-SAM) with respect to enantiomerically-pure L- and D-SAM. (Mean, $n = 2$).

89

Figure 3: FTIR analysis showing the proportion of free amide bonds in drug-free gels, as determined from the band intensity ratio of amide I peaks at 1685 and 1648 cm^{-1} (I_{1685}/I_{1648}), as a function of temperature for gels prepared from 10% *w/w* enantiomerically pure L-SAM (\blacksquare) and racemic D/L-SAM (\square), respectively. (Mean \pm SD, $n = 3$)

90

List of abbreviations

AD	Alzheimer's disease
ANOVA	analysis of variance
BSA	bovine serum albumin
ChEI	cholinesterase inhibitor
DSC	differential scanning calorimetry
FDA	Food and Drug Administration
FTIR	Fourier-transform infrared (spectroscopy)
HA	haemagglutinin
LMW	low molecular weight
LO	lecithin organogel
G'	storage modulus
G''	loss modulus
NMDA	N-methyl-D-aspartate
NMP	nuclear magnetic resonance
NSAID	non-steroidal anti-inflammatory drug
P(MAA-co-MAA)	poly(methacrylic acid-co-methyl methacrylate)
PEO	poly(ethyl oxide)
PLA	poly(lactic acid)
PLGA	poly(lactic acid-co-glycolic acid)
PO	poly(ethylene) organogel
RB	rivastigmine base
RHT	rivastigmine hydrogen tartrate
SAM	N-stearoyl (L-)alanine methyl ester
SC	stratum corneum
SMS	sorbitan monostearate
T _{Gs}	gel-sol transition temperature
T _{SG}	sol-gel transition temperature
v/w/o	vesicle-in-water-in-oil

w/o

water-in-oil

w_o

polar solvent-to-lecithin ratio

Acknowledgements

I thank my research supervisor Dr. Jean-Christophe Leroux for the opportunity (and challenge!) of working in his lab as well as the continued guidance provided throughout the project (especially on the review!). Overall, the past two-something years have been rich in learning, both on professional and personal levels (my understanding of stamina was pushed to new levels). I thank my committee members, Dr. Françoise Winnik and Dr. Didier Hoarau, for their guidance in the bettering of this manuscript. I thank past and present members of the lab, particularly Aude Motulsky, David Ghattas, Anand Dhanikula, Roya Fattahie, Marie-Christine Jones, Marie-Hélène Dufresne, and Guillaume Bastiat, for their general help and the many constructive discussions shared. For backing me with their friendship and advice, my very heartfelt thanks go out to Steven, Irina, Luay, Marie-Eve, Nicolas, and François (my only human partner in the long hours spent with rats). I thank Jean-François for the warmth, love, and patience that make it all seem easy. And last (but n....) I would like to thank my family, Mihaela, Dan, and Razvan, for the unconditional love and support that give me courage to face anything (even grad studies).

Secrétariat du CDEA
Division des animaleries
Pavillon Roger-Gaudry

Renseignements complémentaires au renouvellement autorisé

Protocole 07-099 - Autorisé

Titre : R1-*Pharmacocinétique, biodistribution et efficacité d'immunoliposomes sensibles au pH pour la chimiothérapie de la leucémie myéloïde aigue.*

Directeur de recherche : Dr. Jean-Christophe Leroux

SECTION 9.1 :

Seulement 2 souris ont été utilisées l'année précédente, donc aucune justification sur la justesse des points limites ne peut être rapportée pour le moment.

SECTION 9.2 :

A partir du premier jour d'inoculation des tumeurs, les animaux seront observés attentivement 2 fois par jour afin d'évaluer tout signe de douleur, de stress ou d'inconfort (*i.e.* réduction de l'activité, apparence voûtée, poil ébouriffé et yeux fermés, détresse respiratoire, etc). Les souris seront pesées au moins tous les 2 jours pour évaluer une perte de poids. Si la perte de poids est de plus de 15 à 20 %, les animaux seront sacrifiés. La personne responsable de ce protocole animal est Pierre Simard (étudiant au doctorat) et ce dernier s'assurera de remplir le registre d'utilisation des animaux.

CHAPTER 1

Alzheimer's disease

1. Introduction

Alzheimer's disease (AD) is the most common form of dementia amongst elderly and is estimated to afflict 18 million people worldwide [1]. With an increasingly aging population, the prevalence of AD is on the rise. The disease takes an enormous toll on society, both at financial and social levels. Indeed, about \$100 billion dollars in caring costs are spent annually in the United States alone. Meanwhile, with around 70% of patients living at home, great physical and emotional stress is placed on caregivers [1]. AD is a progressive neurological condition, evolving from short-term memory impairment to profound cognitive disturbances (such as severe memory loss, learning difficulty, and language disorder), behavioural disturbances (such as aggression, depression, and wandering), as well as physical disability [2]. After diagnostic, patients usually survive 7 to 10 years, and typically die from bronchitis or pneumonia [3].

2. Pathophysiology

The disease is characterized, as determined from autopsies, by the extracellular deposition of β -amyloid protein in senile plaques and the intracellular formation of neurofibrillary tangles. The process is thought to be initiated by the production and accumulation of the neurotoxic β -amyloid peptide, the main component of β -amyloid plaques. This leads to the formation of neurofibrillary tangles, oxidation, glutamatergic excitotoxicity, inflammation, and finally an activation of neuronal apoptosis (Figure 1) [4].

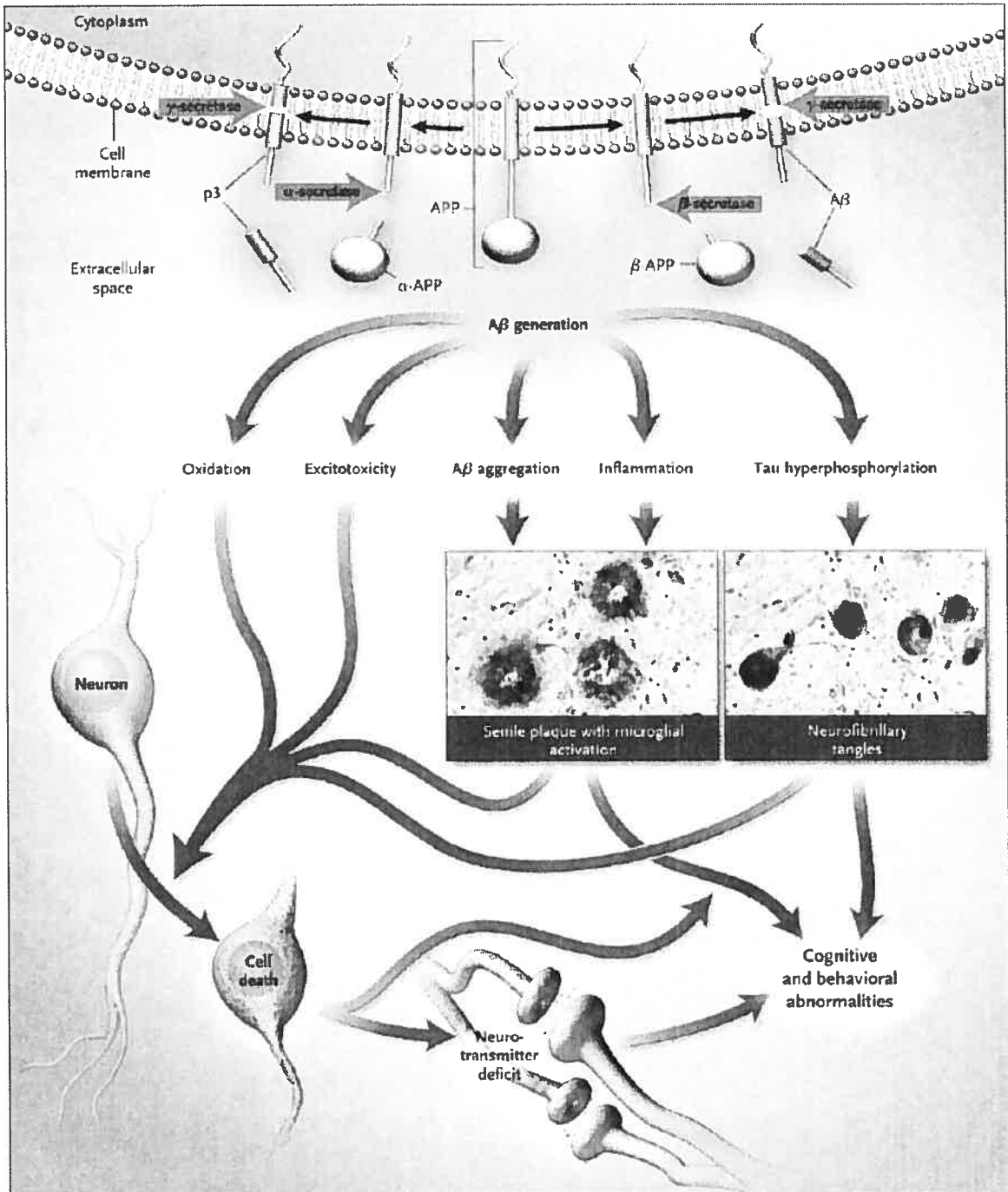


Figure 1: The hypothesis of the amyloid cascade proposes a progression from the generation of β -amyloid precursor protein (APP), through multiple secondary steps, to cell death. Reproduced from reference [4].

3. Treatment options

The cell dysfunction and death brought about in several neurotransmitter systems lead to deficits in acetylcholine, norepinephrine, and serotonin. This hypothesis underlies current pharmacological approaches to the disease (Table I). Amongst these, two classes of drugs are presently on the market, targeting the cholinergic and glutamate systems, respectively. Cholinesterase inhibitors (ChEI) increase acetylcholine levels at synapses by preventing its breakdown, thus prolonging neurotransmission in remaining cholinergic neurons [5], while N-methyl-D-aspartate (NMDA) antagonists are believed to work by regulating levels of glutamate in the central nervous system.

3.1. Cholinesterase inhibitors

Since 1997, three second-generation ChEI have been approved by the Food and Drug Administration (FDA) for treatment of mild to moderate AD: donepezil, rivastigmine, and galantamine (Table I). These agents are currently the first line of symptomatic treatment. Clinical trials have suggested that ChEI may help improve cognitive ability of AD patients. Nevertheless, the overall efficacy of these drugs is generally considered to be modest [4]. Similarly, their slowing of disease progression is controversial [1]. ChEI drugs are generally well tolerated, with possible side-effects of gastrointestinal nature, such as nausea and anorexia. While the three active agents have similar efficacy and tolerability profiles, rivastigmine is the only marketed ChEI that has its effect targeted on the cortex and hippocampus, the areas most affected by the disease.

Table I: Current drugs on the market or in clinical trials for the treatment of AD; adapted from reference [1].

Drug	Company	Mechanism	Status
donepezil (Aricept®)	Eisai/Pfizer	ChEI	approved for mild - moderate AD
rivastigmine (Exelon®)	Novartis	ChEI	approved for mild - moderate AD
galantamine (Reminyl®/Razadyne®)	Johnson & Johnson	ChEI	approved for mild - moderate AD
memantine (Namenda®/Ebixa®)	Lundbeck/Forest	NMDA receptor antagonist	approved for moderate - severe AD
tramiprosate (Alzhemed®)	Neurochem	amyloid plaque inhibition	Phase 3
R-flurbiprofen (Flurizan®)	Myriad Genetics	NSAID ¹ ; lowers β -amyloid levels	Phase 3
leuprolide acetate (Memryte®)	Voyager Pharmaceuticals	Implantable leuprolide	Phase 3
neramexane	Merz & Co	NMDA receptor antagonist	Phase 3
xaliproden	Sanofi-Aventis	5-HT _{1a} agonist	Phase 3
lecozotan	Wyeth	5-HT _{1a} agonist	Phase 3
ispronicline	Targacept/AstraZeneca	nicotinic acetylcholine agonist	Phase 2
bapineuzumab	Wyeth/Elan	β -amyloid-specific monoclonal antibody	Phase 2

¹NSAID: non-steroidal anti-inflammatory drugs

Also, as opposed to donepezil and galantamine, rivastigmine presents a low risk for tolerance caused by enzyme induction and/or upregulation. Likewise, it shows a very low potential for drug-drug interactions and accumulation in the body, even with long-term use [6]. Nevertheless, donepezil, the first second-generation ChEI to enter the

market, has remained the leading product in its class. Antioxidants such as vitamin E are often recommended in conjunction with ChEI up into the late stages of the disease, but this practice is controversial due to the lack of supporting clinical data [1].

3.2. Other therapies

While ChEI are only recommended up to moderate disease stages and have little or no impact on disease progression, the NMDA antagonist memantine, approved by the FDA in 2003, has transformed the treatment of moderate to severe AD. This active agent is thought to interfere with glutamergic excitotoxicity and provide symptomatic improvement through effects on the function of hippocampal neurons [4]. Clinical trials have shown an improvement in cognitive function of memantine- over placebo-treated patients, although as for the other current therapies, improvements remain modest [4]. The potential for combination therapy has been explored, and while some studies have shown encouraging preliminary data, suggesting that treatment with memantine in addition to donepezil is superior to donepezil alone [7], others have concluded that no significant improvement was achieved [8].

While current therapies show modest symptomatic improvements in AD patients, the underlying degeneration of brain cells and consequent disease progression generally remain unaffected by these therapies. Consequently, ongoing research and clinical trials explore new treatment hypotheses (Table I). Several of these agents are aimed at countering amyloid plaque deposition, formation of neurofibrillary tangles, and neuroinflammation. It is argued that the most promising of these avenues is the targeting of the β -amyloid peptide [1]. The most advanced drug in this class is tramiprosate,

which binds soluble β -amyloid, preventing its aggregation into amyloid plaques. Clinical trials revealed the compound to be of moderate efficacy in reducing β -amyloid plaques [9,10]. Another interesting pharmacological approach is represented by bapineuzumab, a humanized monoclonal antibody against β -amyloid, currently studied in Phase 2 trials. Immunotherapy leaves room for hope of a truly disease-modifying approach; however it also entails the greatest risks. Earlier drug candidates have caused cases of encephalitis [1]. It remains to be seen if any of the drugs currently under investigation will provide disease-modifying mechanisms and be safe enough for market release.

Given current pharmacological options for AD patients, a possible way of facilitating disease management could be the administration of sustained release formulations. One example such example has been the commercialization of the oral once-daily formulation of galantamine (Razadyne[®]), an improvement over the previous twice-daily regimen. Simplified dosing schedules could possibly entail increased treatment adherence and compliance, while alleviating responsibility and workload for caregivers. Peak and trough plasma concentrations of the active agent are also potentially minimized, which can decrease side effects.

References

- [1] C. Mount, C. Downton, Alzheimer disease: progress or profit?, *Nat Med* 12 (2006) 780-784.
- [2] J.L. Cummings, G. Cole, Alzheimer's Disease, *JAMA* 287 (2002) 2335-2338.
- [3] R. Brookmeyer, M.M. Corrada, F.C. Curriero, *et al.*, Survival following a diagnostic of Alzheimer disease, *Archives of Neurology* 59 (2002) 1764-1767.
- [4] J.L. Cummings, Alzheimer's disease, *N Engl J Med* 351 (2004) 56-67.
- [5] A. Lleo, S.M. Greenberg, J.H. Growdon, Current pharmacotherapy for Alzheimer's disease, *Ann Rev Med* 57 (2006) 513-533.
- [6] F. Inglis, The tolerability and safety of cholinesterase inhibitors in the treatment of dementia, *Int J Clin Pract Suppl* (2002) 45-63.
- [7] P.N. Tariot, H.J. Federoff, Current treatment for Alzheimer disease and future prospects, *Alzheimer Dis Assoc Disord* 17 Suppl 4 (2003) S105-113.
- [8] A. Enz, C. Gentsch, Co-administration of memantine has no effect on the *in vitro* or *ex vivo* determined acetylcholinesterase inhibition of rivastigmine in the rat brain, *Neuropharmacology* 47 (2004) 408-413.
- [9] S.M. Greenberg, J. Rosand, A.T. Schneider, *et al.*, A phase 2 study of tramiprosate for cerebral amyloid angiopathy, *Alzheimer Dis Assoc Disord* 20 (2006) 269-274.
- [10] P.S. Aisen, D. Saumier, R. Briand, *et al.*, A Phase II study targeting amyloid-beta with 3APS in mild-to-moderate Alzheimer disease, *Neurology* 67 (2006) 1757-1763.

CHAPTER 2

Sustained release systems

Parenteral sustained release systems act as reservoirs for the incorporated active agent, releasing the latter over time spans ranging between hours and months. These systems are generally administered via the peritoneal, subcutaneous, or intramuscular routes, and can be used for systemic or local treatment.

Sustained release systems gained popularity since the early eighties when the first polymeric implants were commercialized for the delivery of goserelin (Zoladex[®]) and levonorgestrel (Norplant[®]), for prostate cancer treatment and contraception, respectively [1]. Microspheres have been developed shortly after for sustained release applications. These systems are constituted of polymeric particles, most commonly polyesters such as poly(lactic acid) (PLA) and poly(lactic acid-*co*-glycolic acid) (PLGA), which are injected subcutaneously or intramuscularly. Microsphere depot formulations containing leuprolide (Lupron[®]) were extensively studied [2] and finally marketed for the long-term release of the active agent with a consequent suppression of testosterone for up to 6 months. A number of studies have investigated the encapsulation of ChEI into biodegradable microspheres of PLA and PLGA [3-6]. These studies showed the potential of drug delivery over prolonged periods. Unfortunately, neither of the model drugs used (huperzine A and tacrine) is commonly used in AD management due to lack of FDA approval and hepatic toxicity, respectively.

Overall, microsphere systems are interesting since many are recognized as being biodegradable and biocompatible [7]. However, important shortcomings of these systems limit their use in drug delivery, notably the complexity of preparation for stable and

sterile formulations and the potential degradation of the active agent during this process. The possibility of microsphere migration away from the injection site can be of nuisance when local treatment is needed. More importantly yet, the formulation cannot be removed in the case of toxic effects following administration. Accordingly, in recent years, such systems have yielded the spotlight to *in situ*-forming systems allowing sustained drug release.

In situ-forming implants are liquid systems which solidify upon injection, as a result of changes in temperature and/or pH, or solvent diffusion [1]. Based on the specific solidification mechanisms, various categories of implants exist, notably thermoplastic pastes, precipitated polymers, hydrogels, and organogels. Each system will be briefly discussed in this section, while organogels will be presented in detail in Chapter 3.

Thermoplastic pastes are composed of polymers which are injected in the molten state and solidify upon injection as a result of temperature drop. These polymers have a melting point between 25 and 65°C and a glass transition temperature below the physiological temperature [8,9]. The latter characteristic is important since the system's viscosity has to present a compromise; while being high enough to provide an adequate rate of release, it must be low enough to permit easy injection through conventional needles [9]. Typical polymers used are composed of lactic and glycolic acids, ϵ -caprolactone, and orthoesters. Poly(ethylene oxide) (PEO) and albumin can be incorporated to provide accelerated release of the active agent. The inherent disadvantage of these systems is the relatively high temperature at which they must be injected. This

can trigger pain and possible necrosis at the administration site. The consequent formation of fibrous tissue around the implant may lead to erratic or insufficient release.

In situ-forming systems can also be produced by chemical or physical crosslinking of polymer chains, yielding solid three-dimensional matrices capable of offering a delaying effect on drug release. The main concern with such systems is the high burst release upon injection, produced by the delay in implant solidification [10]. This is greatly limiting for long-term sustained release applications. Also, polymer crosslinking subsequent to drug incorporation to the formulation involves the risk of chemical modification of the latter and ensuing loss of therapeutic efficacy. Certain formulations have been developed which circumvent this problem, as is the case of a thiol-derivatized poly(ethylene oxide) system which circumvents the need for radical polymerization by allowing crosslinking at the thiol group *via* a linker [11]. However, this formulation is not biodegradable. Finally, another important shortcoming of crosslinked polymer systems is the inherent toxicity of initiators.

As a consequence to the problems associated with chemical crosslinking, polymeric systems relying on solidification triggered by physical interactions seem to be a more reasonable choice for pharmaceutical applications. These systems rely on hydrophobic and/or electrostatic interactions to form the solid systems. The constituting block copolymers contain hydrophilic and hydrophobic parts, which upon a play on temperature and/or pH induce a solidification of the system as a result of altered differential solubilities of the polymer moieties. For example, various such systems are

soluble in cold aqueous media but form a gel upon an increase in temperature. This phenomenon is the result of dehydration of the hydrophobic chain, a consequent loss of solubility in water, and a formation of colloidal systems such as micelles. If colloid density exceeds a given threshold, typically encountered at polymer concentrations of 15-23%, phase mixing occurs between the hydrophilic micelle coronas and the hydrophobic cores, leading to chain entanglement and consequent gelation. [8]. Such polymers most commonly include poloxamers and ABA-type polymers with PEO as the hydrophilic (A) and poly(propylene oxide) as the hydrophobic (B) moiety [12-14]. The major drawback of these systems is the fast release of small hydrophilic molecules through the large aqueous channels formed in the porous implant. Furthermore, poloxamer gels are not biodegradable and have been found to cause metabolic changes in rats [15]. Other thermosensitive di- and tri-bloc copolymers composed of PEO and PLA, PLGA, and/or poly(ϵ -caprolactone) have also been developed in efforts to transcend the problems associated with poloxamer gels [16,17]. These systems were shown to provide adequate release for model drugs, ranging from days to several weeks, for increasingly hydrophobic molecules. A change in pH can also trigger the physical crosslinking of polymers [18,19]. Such systems are mostly used for oral formulations, given the high variations in pH along the gastrointestinal tract.

Finally, the precipitation of compounds as a result of temperature changes or in response to solvent diffusion is also a mechanism exploited for *in situ*-forming systems. An example is Atrigel[®], composed of PLA, PLGA, or poly(lactic acid-co- ϵ -caprolactone) dissolved in N-methylpyrrolidone (NMP). Encouraging animal studies using this system have led to the commercialization of Eligard[®], a formulation providing therapeutic

plasma concentrations of leuprolide in humans for 3 to 6 months [20]. This constituted the first *in situ*-forming implant approved for use in humans. SABER[®] is another system ensuring sustained drug release following *in situ*-precipitation. This formulation is composed of sucrose acetate iso-butyrate, a water-insoluble compound, dissolved in ethanol at concentrations of 80-90% [21]. Injection of the low-viscosity system is followed by solvent diffusion into surrounding tissue and formation of a solid implant capable of providing sustained release of active agents, including proteins, for up to several weeks [21,22].

Organogels, composed of a liquid organic medium immobilized by gelling molecules, are particularly interesting as a drug delivery platform, owing to the simplicity of their preparation. These systems will be discussed in detail in chapter 3, while chapter 4 will focus on the use of an organogel system for the sustained delivery of rivastigmine.

References

- [1] A.J. Tipton, R.L. Dunn, *In situ* gelling systems, in: J. Senior, M. Radomsky (Eds.), Sustained-release injectable products, Interpharm Press, Englewood, 2000, pp. 241-278.
- [2] B.H. Woo, K.H. Na, B.A. Dani, *et al.*, *In vitro* characterization and *in vivo* testosterone suppression of 6-month release poly(D,L-lactide) leuprolide microspheres, *Pharm Res* 19 (2002) 546-550.
- [3] P. Gao, P. Ding, H. Xu, *et al.*, *In vitro* and *in vivo* characterization of huperzine A loaded microspheres made from end-group uncapped poly(d,l-lactide acid) and poly(d,l-lactide-co-glycolide acid), *Chem Pharm Bull* 54 (2006) 89-93.
- [4] X. Fu, Q. Ping, Y. Gao, Effects of formulation factors on encapsulation efficiency and release behaviour *in vitro* of huperzine A-PLGA microspheres, *J Microencapsul* 22 (2005) 705-714.
- [5] W.H. Liu, J.L. Song, K. Liu, *et al.*, Preparation and *in vitro* and *in vivo* release studies of huperzine A loaded microspheres for the treatment of Alzheimer's disease, *J Control Release* 107 (2005) 417-427.
- [6] Q. Yang, D. Williams, G. Owusu-Ababio, *et al.*, Controlled release tacrine delivery system for the treatment of Alzheimer's disease, *Drug Deliv* 8 (2001) 93-98.
- [7] J.M. Anderson, M.S. Shive, Biodegradation and biocompatibility of PLA and PLGA microspheres, *Adv Drug Deliv Rev* 28 (1997) 5-24.
- [8] C.B. Packhaeuser, J. Schnieders, C.G. Oster, *et al.*, *In situ* forming parenteral drug delivery systems: an overview, *Eur J Pharm Biopharm* 58 (2004) 445-455.
- [9] A. Hatefi, B. Amsden, Biodegradable injectable *in situ* forming drug delivery systems, *J Control Release* 80 (2002) 9-28.
- [10] A. Motulsky, Caractérisation d'un organogel à base d'un dérivé amphiphile de la L-alanine, Faculty of pharmacy, University of Montreal, 2005.
- [11] Y. Qiu, K. Park, Environment-sensitive hydrogels for drug delivery, *Adv Drug Deliv Rev* 53 (2001) 321-339.
- [12] M. Katakam, W.R. Ravis, A.K. Banga, Controlled release of human growth hormone in rats following parenteral administration of poloxamer gels., *J. Control. Release* 49 (1997) 21-26.
- [13] M.L. Veyries, G. Couarraze, S. Geiger, *et al.*, Controlled release of vancomycin from poloxamer 407 gels, *Int J Pharm* 192 (1999) 183-193.
- [14] J.G. Wenzel, K.S. Balaji, K. Koushik, *et al.*, Pluronic F127 gel formulations of deslorelin and GnRH reduce drug degradation and sustain drug release and effect in cattle, *J Control Release* 85 (2002) 51-59.
- [15] K.M. Wasan, R. Subramanian, M. Kwong, *et al.*, Poloxamer 407-mediated alterations in the activities of enzymes regulating lipid metabolism in rats, *J Pharm Sci* 6 (2003) 189-197.
- [16] B. Jeong, Y.H. Bae, S.W. Kim, Drug release from biodegradable injectable thermosensitive hydrogel of PEG-PLGA-PEG triblock copolymers, *J Control Release* 63 (2000) 155-163.
- [17] T. Kissel, Y. Li, F. Unger, ABA-triblock copolymers from biodegradable polyester A-blocks and hydrophilic poly(ethylene oxide) B-blocks as a candidate

- for *in situ* forming hydrogel delivery systems for proteins, *Adv Drug Deliv Rev* 54 (2002) 99-134.
- [18] O. Sipahigil, A. Gursoy, F. Cakalagaoglu, *et al.*, Release behaviour and biocompatibility of drug-loaded pH sensitive particles, *Int J Pharm* 311 (2006) 130-138.
- [19] A. Kumar, S.S. Lahiri, H. Singh, Development of PEGDMA: MAA based hydrogel microparticles for oral insulin delivery, *Int J Pharm* 323 (2006) 117-124.
- [20] O. Sartor, Eligard: leuprolide acetate in a novel sustained-release delivery system, *Urology* 61 (2003) 25-31.
- [21] F.W. Okumu, N. Dao le, P.J. Fielder, *et al.*, Sustained delivery of human growth hormone from a novel gel system: SABER, *Biomaterials* 23 (2002) 4353-4358.
- [22] S. Pechenov, B. Shenoy, M.X. Yang, *et al.*, Injectable controlled release formulations incorporating protein crystals, *J Control Release* 96 (2004) 149-158.

CHAPTER 3

Organogels and their use in drug delivery – A review

1. Abstract

Organogels are semi-solid systems, in which an organic liquid phase is immobilized by a three-dimensional network composed of self-assembled, intertwined gelator fibers. Despite their majoritarily liquid composition, these systems demonstrate the appearance and rheological behaviour of solids. Investigative research pertaining to organogels has only picked up speed in the last few decades. Consequently, many burning questions, such as the specific molecular requirements guaranteeing gelation, still await definite answers. Nonetheless, the application of organogels to various areas of interest has been quick to follow their discoveries. Unfortunately, their use in drug delivery is still quite limited by the scarce toxicology information available on organogelators, as well as by the few pharmaceutically-accepted solvents used in gel systems. This review aims at providing a global view of organogels, with special emphasis on the interplay between the gelator's structural characteristics and the ensuing intermolecular interactions. A subsequent focus is placed on the application of organogels as drug delivery platforms for active agent administration *via* diverse routes such as transdermal, oral, and parenteral.

2. Introduction

For the past few decades, gels have been presented, to the extent of a cliché, as being materials “easier to recognize than define”, a prophetic statement pioneered in the 1920’s by Lloyd [1]. Various definitions have followed, sometimes a same author providing descriptions ranging from the most elaborate, stating that a gel 1) has a continuous structure of macroscopic dimensions that are permanent over the time-span of an experiment and 2) is solid-like in its rheological behaviour, to the more basic descriptions stating that if it looks like “Jell-O”, it must be a gel [2]. It is now generally accepted that a gel is a semi-solid material composed of low concentrations (< 15%) of gelator molecules that, in presence of an appropriate solvent, self-assemble *via* physical or chemical interactions into an extensive mesh network preventing solvent flow as a result of surface tension. Gels have been eloquently described as being the result of “crystallization gone awry” [3]. Indeed, macroscopic phase separation into crystalline and liquid layers is avoided in these systems owing to the balance between gelator aggregating forces and solubilizing solvent-aggregate interactions. The result is a system of crystallized fibers that immobilize the liquid phase.

The specific process leading to the formation of the gelling matrix depends on the physicochemical properties of gel components and their resulting interactions. Figure 1 presents a flow-chart compiling various accepted classifications of gels based on the nature of solvents, gelators, and intermolecular interactions.

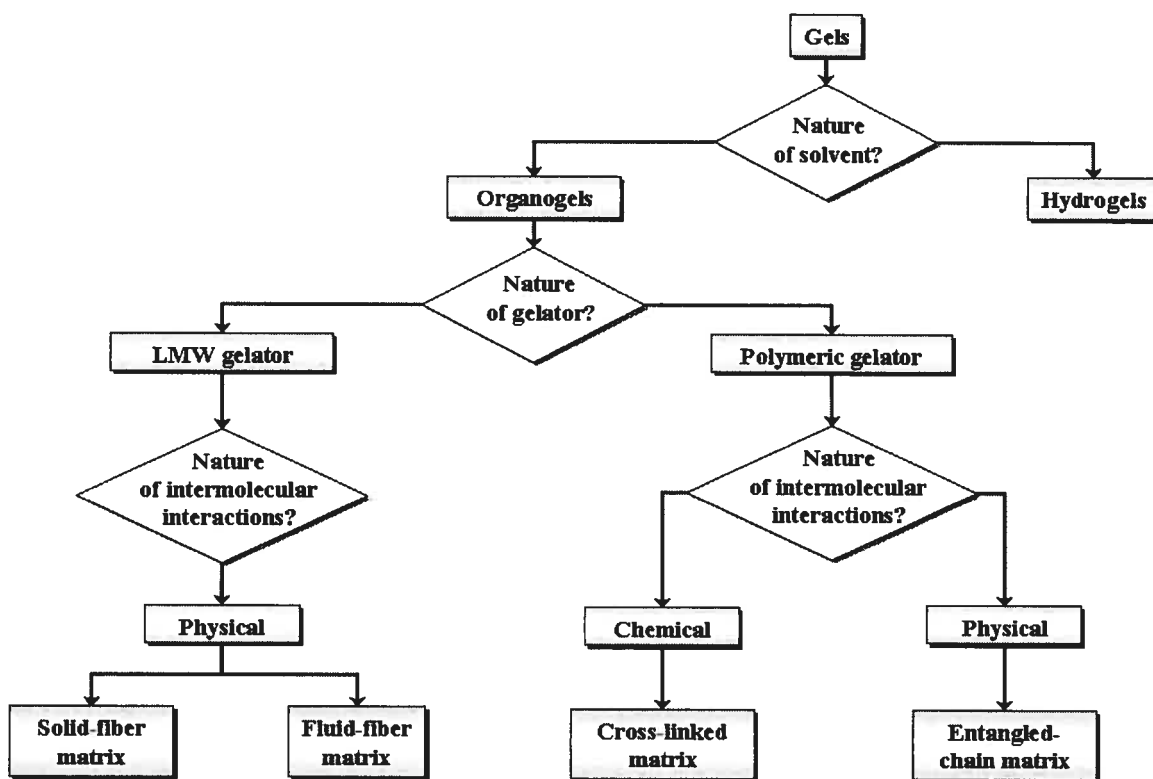


Figure 1: Organogel classification.

Organogels, the focus of this review, can be distinguished from hydrogels by their predominantly organic continuous phase and can then be further subdivided based on the nature of the gelling molecule: polymeric or low molecular weight (LMW) organogelators. Polymers immobilize the organic solvent by forming a network of either cross-linked or entangled chains for chemical and physical gels, respectively. The latter are possibly further stabilized by weak inter-chain interactions such as hydrogen-bonding, van der Waals forces, and π -stacking. Likewise, the self-assembly of LMW organogelators depends on physical interactions for the formation of aggregates sufficiently long to overlap and induce solvent gelation. Depending on the kinetic

properties of aggregates, an important distinction amongst LMW organogels is made between those composed of solid (or strong) *versus* fluid (or weak) fiber networks.

Despite the numerous trends in gelling processes as well as the impressive variety of gelators identified [4], it remains difficult to predict the molecular structure of a potential gelator, as well as one cannot readily foresee preferentially-gelled solvents. Today still, the discovery of gelators remains serendipitous and is usually followed by investigative screening of different solvent systems potentially compatible with gelation. Prediction of gelation potential of a given molecule might seem possible by investigation of its propensity towards chemical or physical intermolecular interactions; however, no generalisations are so far possible. Many factors such as steric effects, rigidity, and polarity can counter the molecule's aggregating tendency. Control over the gelation process as well as the systematic conception of new gelling molecules remain important challenges to face in the quest of new organogelators.

In the pharmaceutical field, organogels can be used for drug and vaccine delivery *via* different administration routes, although relatively few such formulations have been investigated [5]. This review aims in its first part at providing a global view of the different existing organogelator categories while secondly providing a more focused discussion of their drug delivery applications.

3. Organogel properties

3.1. Low molecular weight organogelators

Amongst LMW organogels, a subtle but crucial distinction is made between those composed of entangled networks of solid *versus* fluid fibers (Figure 2) [3].

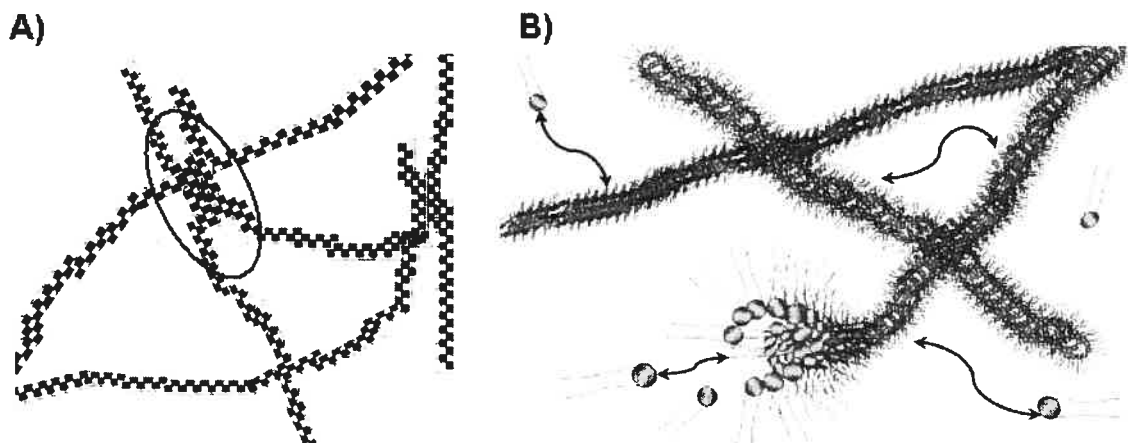


Figure 2: Solid-matrix (strong) *versus* fluid-matrix (weak) organogels. A) Solid-matrix gels are more robust due to their permanent solid-like networks in which the junction points are relatively large (pseudo)crystalline microdomains (circled area). B) Fluid-matrix gels have transient networks in which junction points are most often simple chain entanglements. Additional kinetic features such as dynamic exchange of gelator molecules with the bulk liquid as well as chain breaking/recombination (arrows) may occur. Adapted with permission from reference [3].

The solid fibers, out of which most organogels are composed, are generally produced following a drop in temperature below the gelator's solubility limit [6]. Consequently, a fast partial precipitation of gelator molecules in the organic medium results in the formation of aggregates *via* cooperative intermolecular interactions (Figure 2A) [7]. On the other hand, fluid matrices are formed upon the incorporation of polar solvents to organic solutions of surfactants, which results in the reorganisation of surfactant molecules into mono- or bilayer cylindrical aggregates that immobilize the solvent (Figure 2B) [7]. The key distinction between the two systems is the kinetic stability of

the networks constituting the gel state. Strong gels are formed of permanent, most often crystalline, networks in which junction points are relatively large (pseudo)crystalline microdomains [3]. Conversely, weak gels are formed of transient networks, characterized by the continuous breaking and recombination of the constituent rods, as in the case of reverse cylindrical micelles [8,9]. Similarly, aggregates undergo dynamic exchange of individual gelator molecules with the bulk liquid. Junction points in these fluid networks are simple chain entanglements, equally transient in nature.

The distinction between solid and fluid fibers is not much emphasized in the literature, although it is of great importance from a physicochemical stand point. Solid-matrix gels are more robust, as demonstrated by rheology studies [3]. This may be at least partially due to the fact that, while fluid fibers do not aggregate into higher-order structures, solid fibers are generally aligned in bundles as a result of their rigidity [7], likely conveying added robustness to the gel. Similarly, while molecular and supramolecular chirality plays a great role in the formation and stability of solid fibers, its effect is rare in fluid networks [6,7].

3.1.1. Solid matrix organogels

The vast majority of LMW organogelators discovered so far self assemble into solid networks when added to appropriate organic solvents.

3.1.1.1. General gelling considerations

In merely a century of organogel research, hundreds, if not thousands of LMW molecules with gelling properties have been discovered, most often by chance rather

than design. Several extensive reviews have been published on the topic in general [3,4], as well as on more pointed discussions: fiber formation mechanisms [10] and gelator families derived from various parent molecules such as fatty and amino acids [3], organometallic compounds [3], steroids [3,11], amide- or urea compounds [12], nucleotides [13], and dendrimers [14].

Solid-matrix gels are prepared by dissolving the gelator in the heated solvent, at concentrations typically inferior to 15%. Very low concentrations of less than 0.1% have been reported in the case of sugar-derived “supergelators” [15]. Upon cooling, the affinity between organogelator and solvent molecules decreases and the former self-assemble into solid aggregates held together by intermolecular physical interactions. The remaining solvent-aggregate affinity stabilizes the system by preventing complete phase separation. Aggregates are most often formed by the unidimensional growth into fibers with high aspect (length-to-width) ratios, generally measuring a few tens of nanometers in width and up to several micrometers in length. One such example are L-alanine fatty acid derivatives which form opaque gels in pharmaceutical oils as a result of hydrogen-bonding and van der Waals interactions [16,17] (Figure 3).

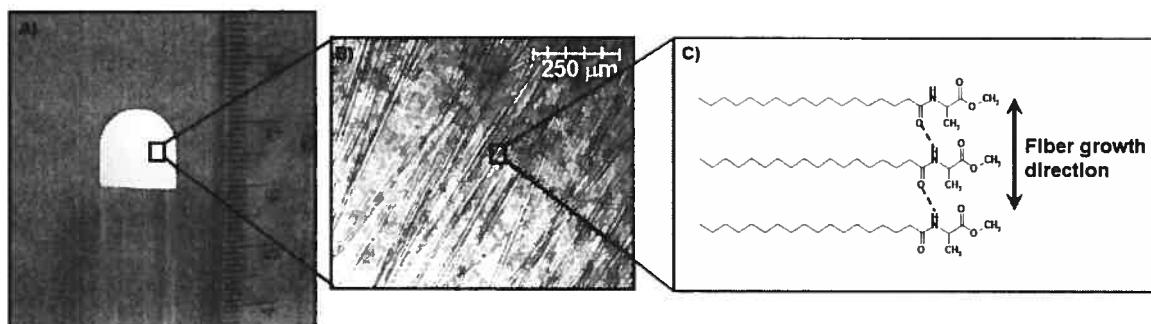


Figure 3: A) Photograph depicting the opaque N-stearoyl-L-alanine methyl ester organogel; B) optical micrograph showing the fibrous aggregates responsible for gelation; C) molecular packing within fibers. Adapted with permission from [18].

Although less common, examples exist of two-dimensional growth patterns, as in the case of hexatriacontane, a 36-carbon n-alkane (C₃₆), which forms microplatelet arrangements (Figure 4).

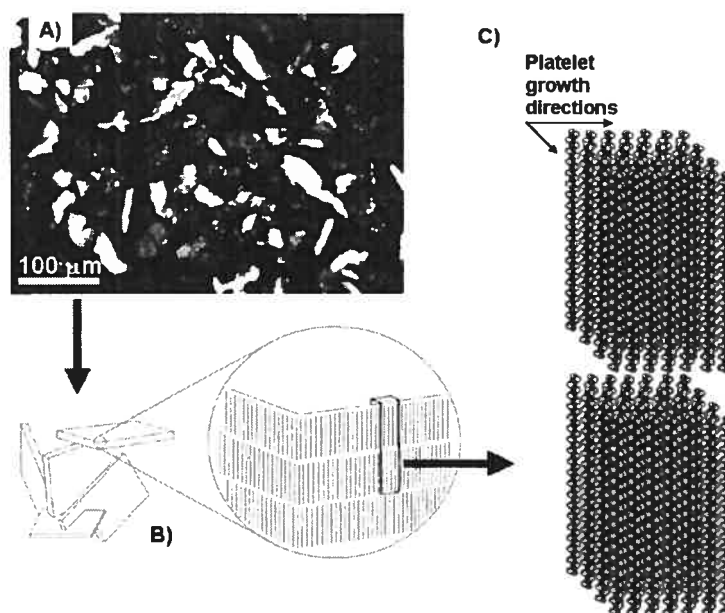


Figure 4: A) optical micrograph of a (4%) hexatriacontane (C₃₆) organogel in octanol viewed through crossed polars; B) a cartoon representation of the microplatelets observed in A); C) depiction of the lamellar orthorhombic molecular packing inside the platelets, showing the directions of microplatelet growth. Adapted with permission from reference [19].

Both one- and two-dimensional aggregates are frequently crystalline in nature. The crystalline arrangement can be the same in the gel and the neat solid, as in the case of C36 molecules, of which the gel microplatelet arrangements are free of liquid molecules in the interlamellar spaces [19]. However, more often than not, the crystalline packing differs between the gel and the neat solid [3]. Macroscopically, organogels range in appearance from white opaque to translucent, likely depending on aggregate size and the consequent gel's ability to scatter incoming light. Sometimes, a same gel system can change in its degree of transparency upon small variations in composition [20].

While hydrophobic attractions are a major driving force for gelator aggregation in water, these interactions are of secondary importance in the case of organogels. In non-aqueous liquids, the attractive forces are mainly hydrogen-bonding, van der Waals interactions, π -stacking, and metal-coordination bonds. Because of the strength and high directionality of their hydrogen-bonds, numerous emerging organogelators are derivatized peptides [4,12], sugars [15,21,22], and bis-urea-based compounds [12]. These are particularly efficient organogelators because of their hydrogen-bonding core that provides a gelling scaffold which can be functionalized for extended versatility. Organogelators consisting of long n-alkanes (chain length varying from 24 to 36 carbon atoms) have proven to be of particular interest in demonstrating the mechanisms of gelation [20]. They are not only rare examples in which hydrogen-bonding does not play a role in gel formation, but are even more unusual in that van der Waals forces alone lead to gelation. As a consequence of gelling solely through these weak physical interactions, such gels are not stable over long periods, eventually phase-separating due

to transitions towards thermodynamically-favoured packing arrangements. Not surprisingly, it was noted that gel shelf-life increased with gelator chain length as a result of extended van der Waals interactions, going from under a day to several months for C24 and C36, respectively [20].

A recent study involving a family of 3,5-diaminobenzoate derivatives demonstrated, although not for the first time, the implication and importance of aromatic stacking in the process of gelation [23]. Indeed, increasingly stronger gels were formed upon incorporation of additional aromatic substituents to gelator molecules. Another interesting class of gelators involving π - π interactions are cholesterol-derivatized molecules. These can be very suitable for the design of functionalized organogelators because of their remarkably high synthetic tunability [3,11]. The cholesterol group induces uni-directional self-association through van der Waals interactions, while functional groups added onto the cholesterol backbone stabilize the fiber *via* hydrogen-bonding and/or π - π interactions. The hydroxyl group at the C3 position of the cholesterol molecule is crucial to gelation, likely due to its participation in hydrogen-bonding [3]. Alternatively, steroids (S) derivatized at the C3 position with anthraquinone (A) *via* a linker (L) of varying length (ALS compounds) are known to form stable organogels. The fused aromatic rings of the anthraquinone group stabilize gel fibers by π -stacking.

3.1.1.2. Chirality Effects

Chirality is neither necessary nor sufficient for gelation; however, despite not being a gelling-force in itself, chirality seems to be intimately related to the growth and stability of the self-assembled fibrillar networks of LMW physical gels [3]. While this section strives at providing the reader with a general view of underlying principles of chirality and their impact on gelation, more extensive information can be found in a recent and excellent review by Brizard *et al.* [6].

Although the exact explanation remains yet to be formulated, a general empirical rule is that a molecule has a better chance of being a good gelator if it is chiral. Indeed, a large majority of existing organogelators possess at least one stereogenic center, while non-chiral gelators are generally cited as being exceptions to the rule [6]. Furthermore, it can be specified that chirality is only determinant in the case of solid fibers due to their marked rigidity, while rarely being of effect in fluid fibers which are highly dynamic in nature [7].

To further understand the stabilizing effect of chirality, it must first be said that it is known to play important roles both at the scale of individual molecules as well as that of resulting fibrillar aggregates. Indeed, molecular chirality is most often transferred to the morphology of self-assembled fibers, as shown by numerous studied systems [24-28]. One such example are crown ether phthalocyanine organogels, composed of supercoiled helical fibers (Figure 5).

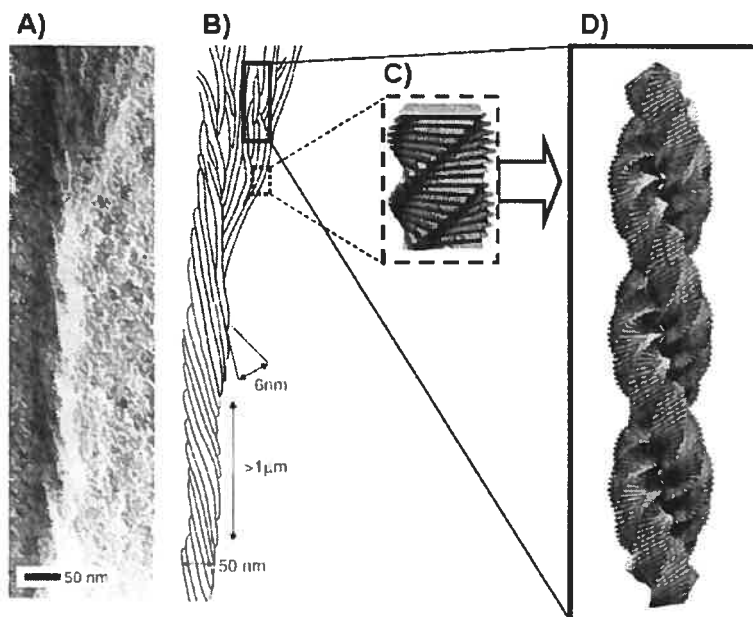


Figure 5: A) Transmission electron micrograph of organogel of a crown ether phthalocyanine in chloroform, showing a left-handed coil. B) Schematic representation of helical fibers in A). C) The helical aggregates are formed by the stacking of crown ether rings with a staggering angle, constant in magnitude and direction. D) Supercoiled structure is obtained from side-on aggregation of individual fibers. Reproduced with permission from reference [27].

Initial molecular packing, driven by π -stacking between substituent aromatic rings, transfers molecular chirality to individual fibers, which further twist around each other into helical superstructures to maximize van der Waals interactions [27]. As opposed to flat aggregates, the contact area between such twisted structures is reduced due to their curvature, which makes them less prone to uncontrolled aggregation and to the resulting precipitation. This increases the chance of gelation by such chiral molecules. The opposite is generally true of racemic mixtures. These most often form flat aggregates that are more prone to uncontrolled crystallization [24,29].

N-stearoyl alanine methyl ester is an example of a compound showing superior gelling abilities when enantiomerically pure. Such gels exhibited higher transition temperatures than their racemic counterparts (Figure 6) [30].

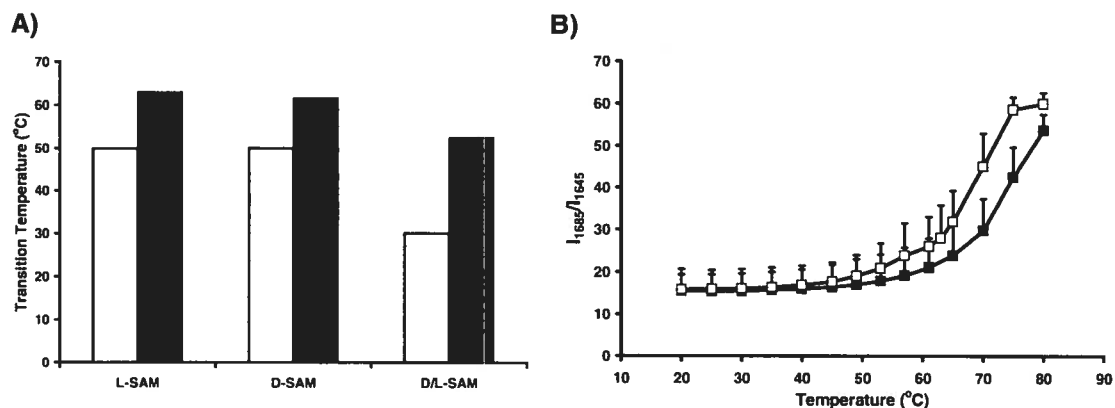


Figure 6: A) Gelator chirality effect showing a decrease in DSC-determined sol-gel (white bars) and gel-sol (solid bars) transitions in racemic organogels (N-stearoyl D/L-alanine methyl ester, D/L-SAM) with respect to enantiomerically-pure L- and D-SAM organogels, respectively (mean, $n = 2$). B) FTIR analysis showing the proportion of free gelator amide bonds in gel systems, as determined from the band intensity ratio of amide I peaks at 1685 and 1648 cm^{-1} (I_{1685}/I_{1648}), as a function of temperature. Enantiomerically pure L-SAM (■) organogels showed higher gel-sol transition temperatures than D/L-SAM (□) organogels (mean \pm SD, $n = 3$) [30].

Meanwhile, racemic mixtures are often reported to form weaker gels, to crystallize [24], or to precipitate as flakes or pellets [6]. Nevertheless, a few examples have been reported in which racemates actually form stronger and/or more stable gels than their enantiomerically pure analogues, demonstrating that although racemates are often poorer gelators, this empirical observation cannot be taken as a rule [6].

3.1.2. Fluid-matrix organogels

Fluid fibers gel organic solvents in much the same way as solid fibers: aggregate size increases and the eventual entanglement of these structures immobilizes the solvent as a result of surface tension. Just as strong gels, fluid matrix systems are thermoreversible and can be transparent or opaque. The critical difference arises in the kinetic behaviour of the two types of matrices. While solid matrices have a robust and permanent morphology over the gel's lifespan, fluid matrices are transient structures in constant dynamic remodelling (Figure 2) [3]. Owing to the aggregate fluidity and the transience of junction points, these structures are also referred to as "worm-like" or "polymer-like" networks. This section presents two such systems, lecithin and sorbitan monostearate (SMS) (and/or sorbitan monopalmitate) organogels, which are both of very high interest in pharmaceutical sciences.

3.1.2.1. *Lecithin organogels*

From a drug delivery standpoint, lecithin organogels (LO) are very interesting systems, owing to their biocompatibility, their amphiphilic nature, facilitating dissolution of drugs of various classes, as well as their permeation enhancement properties. Lecithin, or phosphatidylcholine (Table I), is the most abundant phospholipid in biological systems and is typically extracted from soy beans and egg yolk. Due to its amphiphilic structure, lecithin can assume many different forms such as mono- and bi-layer films, vesicles, liquid crystals, emulsions, and organogels [9]. When mixed to organic solvents, lecithin yields isotropic reverse-micellar solutions. Upon the addition of small amounts of polar solvents, cylindrical reverse micelles start to grow until they entangle into a gelling network (Figure 7).

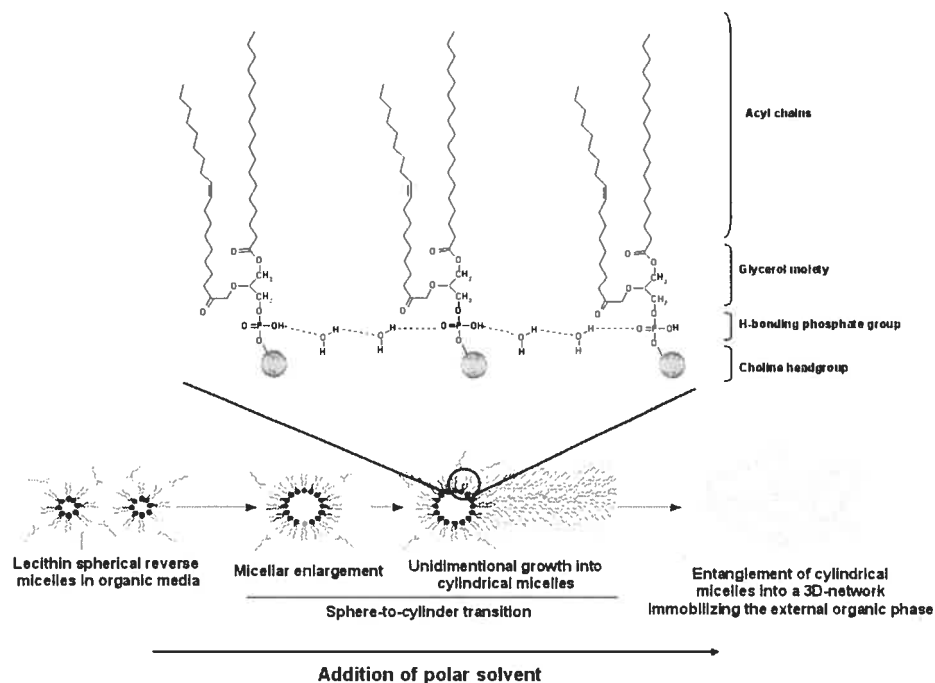


Figure 7: Formation of a three-dimensional network of reverse cylindrical micelles in lecithin organogel, involving hydrogen bonding between lecithin and polar solvent molecules. Adapted with permission from reference [31].

Despite having been termed “weak” organogels, LO present very high viscosities, in several cases higher than that of gelatin [32]. Scartazzini *et al.* [32] were the first to report a systematic investigation of LO, their results subsequently confirmed by several groups. Indeed, evidence was presented suggesting that the rise in the systems’ viscosity was due to the growth and overlap of reverse tubular micelles [33-35] and not to any form of liquid crystalline order [33], as in the case of binary water-lecithin systems [9].

The hypothesis of entangled reverse micelles was proven by infrared spectroscopy studies showing a low-frequency shift of the P=O vibration band for lecithin molecules upon gel formation, indicating the involvement of the phosphate group in H-bonding with the added polar solvent [34,36]. No indications were found of interactions at the

carbonyl groups and the glycerol residue of lecithin. Based on this evidence, a structural model was proposed, in which the lecithin phosphate group and polar solvent molecules are connected by H-bonds, thus forming a linear structure of alternating solvent and lecithin molecules, which ultimately self-assembles into overlapping worm-like reverse-micelles (Figure 7). Corroborating NMR studies [37-40] showed a line broadening for phosphorous and hydrogen resonances of the polar head-group upon an increasing molecular ratio of solvent-to-lecithin (w_o). This suggested a progressive molecular stiffening of this part of the molecule upon polar solvent addition, consistent with the hypothesis of inverted cylindrical micelle formation and entanglement.

Several polar solvents, many suitable for *in vivo* use, were found appropriate for induction of gelation. Glycerol provided maximal viscosity of the ternary system at the lowest concentration ($w_o = 1.7 - 1.9$), followed by water ($w_o = 3.6 - 3.8$), formamide ($w_o = 3.6 - 4.8$), and ethylene glycol ($w_o > 5$) [34]. Other solvents such as ethyl alcohol and diethylene glycol did not induce organogel formation. In fact, it was suggested that the difference between gel-forming and non-gel-forming solvents was their orientation and localization between lecithin molecules, which in turn depended on their polarity [36]. Similarly, all gelling-solvents were found to have a strong tendency towards hydrogen-bonding, with hydrogen-bond donating potential seeming to be more important than hydrogen-bond acceptance. In terms of the hydrophobic organic solvents compatible with gel formation, Scartazzini *et al.* [32] concluded that the more apolar solvents such as alkanes, followed by cycloalkanes, allow a higher state of structural organization of the lecithin molecules, thus forming more stable gels.

Phase diagrams were obtained by several groups, describing the variation of the lecithin system viscosity with the addition of increasing amounts of polar solvent. They remained relatively constant for all hydrocarbon solvents used [33,34,36] (Figure 8).

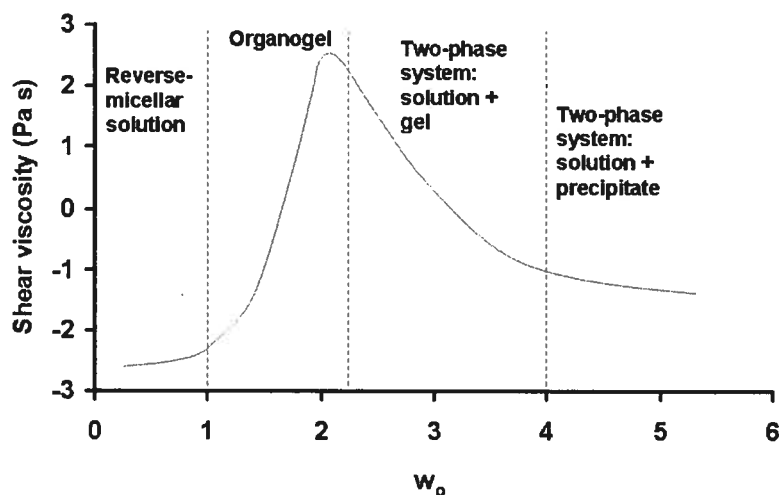


Figure 8: Plot of zero shear viscosity *versus* the water-to-lecithin molecular ratio (w_0). Dotted lines roughly indicate boundaries between various phase regions. Adapted with permission from reference [36].

Slight variations occurred for certain other organic solvents [41], but the evolution of the lecithin system structure upon addition of polar solvent is a constant. The initial lecithin reverse-micelle solution always presents a sharp increase in viscosity upon the addition of critical amounts of water, coinciding with organogel formation. Further addition of water leads to a sharp decrease in viscosity, owing to the separation of a homogenous gel from the remaining low-viscosity fluid. Finally, the solidification of the separated gel into a non-transparent solid precipitate occurs at even higher concentrations of polar solvent. More extensive physicochemical characterization can be found in the review by Shchipunov [42].

3.1.2.2. Fatty acid derived organogels

Other biocompatible organogels extensively investigated in drug delivery are SMS (Span 60) and sorbitan monopalmitate (Span 40) organogels (Table I). Murdan *et al.* [43-46] were the first to report organic solvent gelation by these two compounds, both in the presence and absence of an aqueous phase. Anhydrous gels were obtained by dissolving low concentrations (1-10%) of the organogelator in alkanes ($C > 5$), isopropyl myristate, and various vegetable oils at 60°C. Subsequent cooling of the system yielded white thermoreversible gels at room temperature. Alternatively, the drop-wise addition of an aqueous phase, in the form of either water or a suspension of niosomes (surfactant bilayer vesicles) to the hot organic surfactant solution yielded upon cooling a water-in-oil (w/o) or a vesicle-in-water-in-oil (v/w/o) organogel system, respectively.

As with all gelling mechanisms, the gelation point corresponds to decreased solvent-gelator affinities resulting in a structural transition, in this case from the isotropic phase composed of reverse micelles to a system of entangled rod-shaped tubules that immobilizes the solvent [46,47]. Further organization of the amphiphiles inside the tubules was suggested to consist of concentric inverted bilayers, which as in the case of LO were found to be stabilized by hydrogen bonds between water and the amphiphiles' polar heads [44,46,48].

The classification of these non-ionic surfactant organogels as either solid- or fluid-matrix systems is less clear-cut than in the preceding cases. Although the bilayer arrangement within tubules intuitively suggests a certain fluidity and possible exchange of surfactant molecules with the surrounding bulk liquid, certain studies tend to point

away from the fluidity hypothesis. Indeed, when viewed under polarized light, the tubular aggregates exhibited crystallinity [48]. Nevertheless, X-ray diffraction measurements have shown the inverted bilayers to increase in width upon the addition of water, suggesting the accommodation of the aqueous phase between opposing polar groups of the amphiphilic bilayer [44] pointing towards the plasticity of the systems. A saturation point was reached, after which excess water accumulated in separate droplets bound by surfactant film at the interface, followed by the eventual breakdown of the gel as aggregate integrity is substantially lost. The continuous modulation of the system to accommodate the polar solvent suggests a dominating fluid character for the constituting matrix.

3.2. Polymeric gelators

Polymeric gelators behave similarly to their LMW counterparts, solidifying organic solvents based on physical intermolecular interactions. Polymeric gels can vary from linear to star-shaped polymers. Three such polymeric systems with common or potential uses in drug delivery will be presented in this section.

Poly(ethylene) organogels (PO) are commonly used as ointment bases and are composed of 5% low molecular weight poly(ethylene) in mineral oil (Plastibase[®]) (Table I) [49-51]. The polymer is dissolved in the oil at about 130°C and “shock-cooled”. This leads to the partial precipitation of the polymer chains and the formation of a colorless organogel [49-51]. Also of common application in pharmaceuticals are copolymers of methacrylic acid (MAA) and methyl methacrylate (MMA) in 1:1 (Eudragit L[®]) and 1:2 (Eudragit S[®]) molar ratios (Table I). These can be used in the preparation of organogels

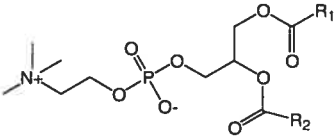
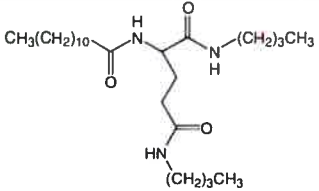
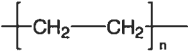
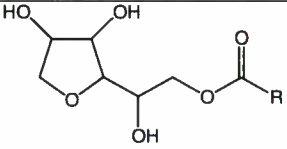
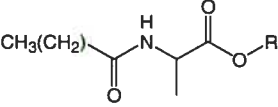
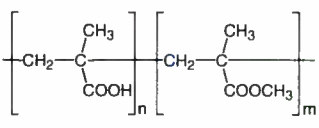
that have been evaluated as rectal sustained release preparations [52,53]. In the available studies, such gels typically consisted of a model drug dissolved in propylene glycol containing high concentrations of the gelling polymer (30 and 40 % for 1:1 and 1:2 P(MAA-*co*-MMA), respectively). Basic drugs were found to weaken the gel structure more than acidic drugs, a phenomenon attributed to an increased disturbance of the hydrogen-bond interactions between polymer and propylene glycol molecules by the former.

Recently, Jones *et al.* [54] presented the preparation of star-shaped alkylated poly(glycerol methacrylate) amphiphiles, capable of forming polymeric micelles in pharmaceutically-acceptable apolar solvents such as ethyl oleate. It was found that organogel formation occurred at high polymer concentrations ($> 10\%$) when the latter were derivatized with medium-length C_{12} and C_{14} alkyl chains. On the other hand, gelation occurred at much lower concentrations ($\leq 1\%$) in the case of C_{18} -derivatized polymers, showing the importance of intermolecular van der Waals interactions in the gelation mechanism. Hydrogen bonding *via* the hydroxyl groups of the core polymers was suggested to be a driving force for gelation. The systems were shown to increase the solubility of hydrophilic compounds in oils, making them potentially useful for the preparation of anhydrous peptide formulations. Potential drug delivery from these organogels remains an interesting option to be explored.

4. Organogels in drug delivery

Despite the large abundance and variety of organogel systems, relatively few have current applications in drug delivery, owing mostly to the lack of information on the biocompatibility and toxicity of organogelator molecules and their degradation products. This section focuses on organogel systems that have been geared towards pharmaceutical applications and are at various stages of development, from preliminary *in vitro* experiments to clinical studies. Table I provides a summary of the key drug delivery studies conducted using organogels.

Table I: Organogel formulations used in drug delivery

Organogelator used in formulation	Route of administration	Study conducted	Model drugs	
Lecithin  R_1 and R_2 = various fatty acids of which linoleic (55%) and palmitic (13%) acids	Transdermal	Clinical trials <i>In vivo</i> skin permeation and efficacy <i>In vitro</i> skin permeation <i>In vitro</i> release	Diclofenac [55-57] Piroxicam [58] Tetrabenzamide [59] Scopolamine and Boxaterol [39] Propranolol [60] Nicardipine [61] Aceclofenac [62] Indomethacin and Diclofenac [63]	
Glyceryl fatty acid esters	Mixture of mono-, di-, and tri-glycerides of C_{16} and C_{18} fatty acids	Transdermal	<i>In vivo</i> efficacy	Levonorgestrel and Ethinyl estradiol [64]
N-lauroyl-L-glutamic acid di-n-butylamide		Transdermal	<i>In vitro</i> release	Haloperidol [65,66]
Poly(ethylene)		Transdermal	<i>In vitro</i> release	Spectrocin [49]
Sorbitan monostearate (SMS) or molaureate	 $R = (CH_2)_{16}CH_3$ or $(CH_2)_{10}CH_3$	Nasal Oral Subcutaneous and intramuscular	<i>In vitro</i> release <i>In vitro</i> release <i>In vivo</i> efficacy	Propranolol [67] Cyclosporin A [68] BSA ¹ and HA ² [43,44,69]
N-stearoyl L-alanine methyl or ethyl ester	 $R = CH_3$ or CH_2CH_3	Subcutaneous	<i>In vitro/in vivo</i> release <i>In vitro/in vivo</i> release and efficacy	Rivastigmine [18] Leuprolide [70]
P(MAA-co-MMA) ³		Rectal	<i>In vivo</i> efficacy	Salicylic acid
P(MAA-co-MMA) and cPAA ⁴		Buccal	<i>In vivo</i> efficacy	BSA ¹

¹ BSA: bovine serum albumin (antigen model)² HA: haemagglutinin (antigen model)³ P(MAA-co-MMA): poly(methacrylic acid-co-methylmethacrylate)⁴ cPAA: crosslinked poly(acrylic acid)

4.1. Dermal and transdermal formulations

Drug delivery into the skin layers (cutaneous or dermal delivery) and beyond (percutaneous or transdermal delivery) is advantageous because it provides a non-invasive, convenient mode of administration without the first pass degradation of the active ingredient, an important aspect for highly liver-metabolized molecules [61]. Despite the great potential of dermal and transdermal drug delivery systems, relatively few drugs are available as topical formulations. The difficulty in developing such systems lies mostly in the circumvention of the barrier properties of the stratum corneum (SC). Nevertheless, with absorption issues at least partially circumvented by the use of permeation enhancers, a number of vehicles, of which organogels, have been developed for transdermal delivery [31]. An important advantage of such systems is their general ease of preparation, the latter typically consisting in simple dissolution of drug and gelator in the liquid medium.

An important class of permeation enhancers with wide use as organogel components are saturated and unsaturated fatty acids [71]. Amongst these, oleic acid and isopropyl palmitate are particularly interesting for their common use in organogels. It is thought that the precise mechanism of action is the penetration of the fatty acid moieties into the lipid bilayers of the SC and the consequent creation of separate domains which become highly permeable pathways [72].

Surfactants [71,73] and phospholipids [74] constitute another class of molecules proven to possess permeation enhancing properties. These compounds likely absorb into the SC and increase tissue hydration, consequently increasing drug permeation in the case of

hydrophilic active agents. Fluidisation of the lipid bilayer, with eventual extraction of lipid components is also thought to occur for both surfactants [72,75] and phospholipids [63,76,77].

Despite the presentation of these generalized trends, it should be said that permeation enhancing properties are highly dependent on the overall formulation and more specifically on the physicochemical properties of the permeating drug molecule [78]. Caution should therefore be employed in drawing conclusions about particular systems solely based on the potential effects of individual components.

4.1.1. Lecithin

The most investigated organogels for topical delivery are LO (Table I); a recent review published on the topic provided a relatively exhaustive list of active agents loaded in such formulations [31]. LO present several favourable characteristics for transdermal delivery owing to their amphiphilic nature. Firstly, the lecithin and oil can efficiently partition with the skin and provide an enhanced permeation as has been shown for several model drugs [39,60-62]. The effect was attributed to both the solvents used (isopropyl palmitate, ethyl oleate, etc.) [63] as well as to the lecithin itself [58,60]. The amphiphilic nature of LO also allows solubilization of guest molecules in either the organic or aqueous phase, thus permitting the incorporation of molecules with diverse physicochemical character, such as vitamins A and C [32], as well as peptides [39].

In the case where a therapeutic effect is needed in a localized region close to the skin surface, transdermal delivery offers net advantages over oral administration, mainly in

terms of lowered systemic side-effects. This potential advantage has been nicely demonstrated for LO in several laboratories and clinical studies. Nastruzzi *et al.* observed a levelling in subcutaneous tumour growth in mice treated transdermally with a LO containing an anti-tumoral agent (tetra-benzamidine) [59]. When the LO was applied away from the affected region, the tumour continued to grow, demonstrating lower systemic *versus* local effects of the system. Similarly, the incorporation of non-steroidal anti-inflammatory drugs (NSAIDs) into LO has been given particular attention because of the potential to apply the analgesics close to the site of action, as could be useful in the case of rheumatism. With these scopes in mind, transdermal delivery of NSAIDs (aceclofenac [62] and piroxicam [58]) from LO was demonstrated in standard permeation studies. Also, several double blind, randomized clinical trials on patients suffering of various musculoskeletal ailments (orthoarthritis, lateral epicondylitis, sprains, etc.) and treated transdermally with 1-2% diclofenac in LO, revealed significant improvements in terms of analgesic efficacy compared to placebo [55-57].

Histological studies on excised human skin showed no toxic effects when LO were applied to the skin for prolonged periods of time [39]. In a study on over 150 volunteers, acute irritation attributed to LO application was rare and discrete. Similarly, a low cumulative irritancy potential was demonstrated (IT_{50} , irritation time of 50% of the test population, equal to 13 days) [79]. Overall, LO are currently the most advanced of all LMW organogel systems; LO ointment bases are commercially available for magistral preparations [55].

4.1.2. Fatty acid-derived sorbitan organogels

Organogels consisting solely of non-ionic surfactants (prepared by dissolving 20% SMS in liquid surfactants, *e.g.* polysorbate 20 or 80) were tested for their safety as topical formulations [73]. The surfactants being known permeation enhancers, adverse effects resulting from modifications in skin structure were investigated on shaved mouse as well as on human skin. In both cases, no significant increases in blood flow and in epidermal irritation was observed. Some epidermal thickening was however noticed, suggesting a marked interaction between the surfactants and SC components. Overall, the gels were regarded as safe and well-tolerated by volunteers when applied daily for 5 consecutive days. However, to the best of our knowledge, no skin permeation or efficacy studies using these organogels have been published to date.

4.1.3. Organogels based on other low molecular weight gelators

Pénzes *et al.* investigated the transdermal delivery of piroxicam from organogels composed of glyceryl fatty acid ester gelators in pharmaceutical oils [80,81]. The *in vivo* skin penetration of the drug, evaluated by measuring the anti-inflammatory inhibition of oedema after treatment, was found to be superior for glyceryl fatty acid ester organogels as compared to traditional topical formulations such as liquid paraffin [81]. Chan *et al.* [65,66] reported the use of a long acyl-chain glutamate-based gelator (N-lauroyl-L-glutamic acid *di-n*-butylamide) at concentrations of 2-10% to gel isostearyl alcohol and propylene glycol, yielding translucent and opaque gels, respectively. *In vitro* permeation studies on human skin using haloperidol, an anti-psychotic drug, showed facilitated permeation upon incorporation of 5% limonene, a known permeation enhancer.

4.1.4. Poly(ethylene) organogels

Contrary to hydrogels [82-85], very few polymeric organogels have been geared to pharmaceutical applications. The only two such systems having been widely tested for drug delivery applications are poly(ethylene) and P(MAA-*co*-MMA) organogels.

In a study dating back to the 1950s and involving 300 patients, PO patches were shown to be non-irritating and to have low sensitizing properties [49]. In a related investigation, 326 patients were treated with spectrocin-containing PO and compared with patients treated with spectrocin in petrolatum base alone. Both antibiotic ointments cleared pyoderma and secondarily infected eruptions in 3-5 days, but it was found that the PO provided a faster, more efficient release. Poly(ethylene) was also used in the formulation of 5-iodo-2'-deoxyuridine for the treatment of oral herpes simplex lesions. A 10% drug-loaded formulation showed a resolution of herpetic lesions in 3-days after treatment initiation, compared to 1-2 weeks in untreated control patients [50]. Similarly, PO were employed as a base for a patch testing metal allergens [51]. The bioavailability of nickel antigens from the PO patch applied to the back of patients was found to be as good as for the control methylcellulose patch.

4.2. Parenteral depot formulations

Anhydrous and water-containing organogels were formulated for depot formulations using SMS and different gelation modifiers (polysorbates 20 and 80) in various organic solvents and oils. These gels were shown to be suitable for the controlled release of drugs and antigens.

SMS organogels containing either w/o or a v/w/o emulsions were investigated *in vivo* as delivery vehicles for vaccines using bovine serum albumin (BSA) and haemagglutinin (HA) as model antigens [43,44,69]. Intramuscular administration of the v/w/o gel yielded the longest-lasting depot effect (48 h). This could be readily explained by the combined barriers to diffusion present in this formulation (niosomes and gel matrix) [69]. Nevertheless, the release was relatively short-lived, likely due to the percolation of interstitial fluid into the gel, causing it to fragment and emulsify [45]. Based on the observed phenomena, the release mechanism for hydrophilic antigens was assumed to be driven by gel disintegration. The studies also showed that both the w/o and v/w/o gels possessed immunoadjuvant properties and enhanced the total primary and secondary antibody titres to the HA antigen in mice.

Controlled release of the contraceptive steroids levonorgestrel and ethinyl estradiol was achieved by Gao *et al.* from subcutaneously-injected biodegradable organogel formulations prepared from glyceryl ester fatty acids in derivatized vegetable oil [64]. Despite an inflammatory reaction in injected rats lasting up to 7 days, the gel formulations proved their efficacy by completely blocking the estrous cycle of female rats up to 40 days. The duration of the biological effect was of the same order of magnitude as the time needed for gel degradation, suggesting the latter phenomenon to control drug release from the implant.

Subcutaneously-injected *in situ*-forming organogels prepared from L-alanine derivatives in safflower oil were used in the long-term delivery of leuprolide, a luteinizing hormone-releasing hormone agonist used in prostate cancer [70]. The gels were shown to slowly

degrade and release the therapeutic peptide for a period of 14 to 25 days. The efficacy of the system was demonstrated by the induced chemical castration (inhibition of testosterone secretion), lasting up to 50 days (Figure 9). More recently, the same systems, using the N-stearoyl L-alanine methyl ester organogelator in safflower oil, were used in the sustained delivery of rivastigmine, a cholinesterase inhibitor used in the treatment of Alzheimer's disease [18]. Following subcutaneous injection, the oleogels provided a 5-fold lower burst effect than control oil formulations, followed by sustained release of the drug for up to 11 days. Histology studies showed these organogels to have a good biocompatibility profile over an 8-week evaluation period [16]. Overall they represent a promising platform for long-term sustained drug delivery.

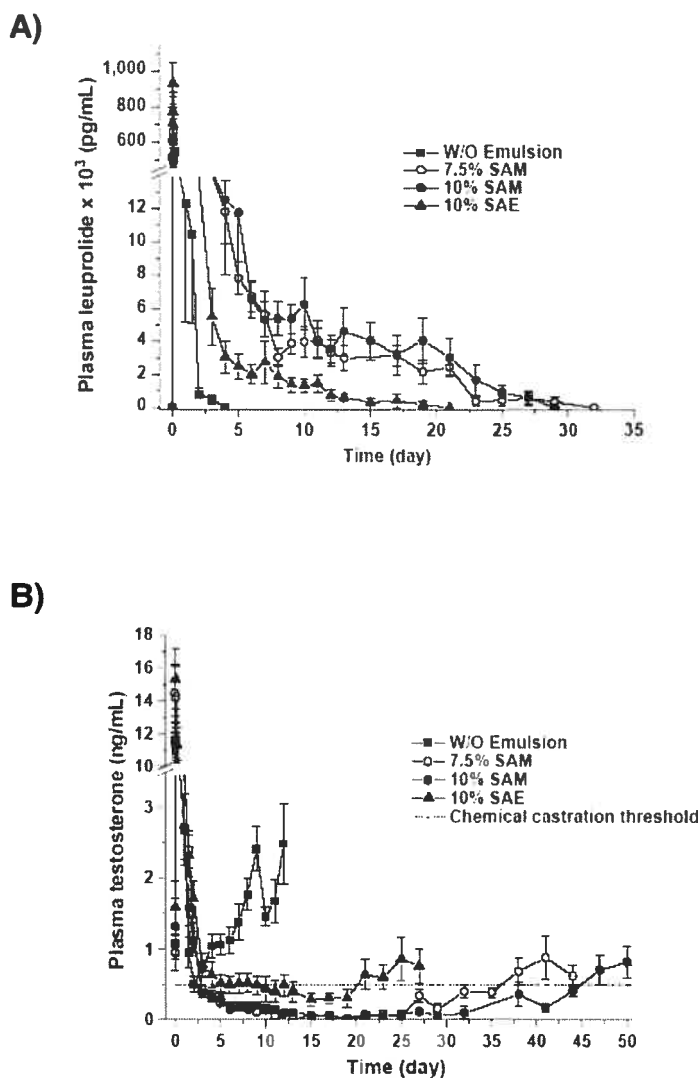


Figure 9: A) Plasma concentrations of leuprolide after the subcutaneous administration of a control w/o emulsion (squares) and various organogel formulations (circles and triangles; SAM and SAE: N-stearoyl methyl or ethyl ester, respectively). B) Plasma concentrations of testosterone after the administration of the formulations in a). The dotted line represents the chemical castration threshold (mean \pm SEM, n=5-6). Reproduced with permission from reference [70].

4.3. Oral and trans-mucosal formulations

The only example found in the literature of oral organogel formulations was that of SMS systems recently investigated by Murdan *et al.* [68]. Cyclosporin A, a powerful

immunosuppressant used after organ transplantation, was incorporated in organogels varying in nature from highly hydrophobic (SMS in sorbitan monoleate) to more hydrophilic systems (SMS in polysorbate 80). Upon administration to beagle dogs, the hydrophilic organogels allowed less drug absorption than the hydrophobic formulations, likely due to the absence of lipophilic domains in which the drug could remain soluble once in contact with the aqueous gastric medium. The hydrophobic organogels showed absorption profiles similar to those of the commercially available Neoral[®] microemulsion formulation.

Organogels composed of P(MAA-*co*-MMA) have been tested as suppository formulations. *In vitro* dissolution patterns of salicylic acid from organogels composed of 1:1 and 1:2 P(MAA-*co*-MMA) (Eudragit L[®] and Eudragit S[®], respectively) [53] showed an initial burst of drug release in both cases, followed by a slow release phase. Salicylic acid followed a zero-order release from 1:1 P(MAA-*co*-MMA) organogels, providing strong evidence for a surface erosion release mechanism with negligible diffusion. On the contrary, the same drug was released from 1:2 P(MAA-*co*-MMA) organogels in a linear function *versus* the square root of time, suggesting a diffusion-controlled release mechanism. Although an explanation was not provided by the authors, it can be hypothesized that this difference in release profiles is due to the relative hydrophilicity of the two copolymers. The more hydrophilic 1:1 copolymer allows more water penetration into the gel matrix, giving rise to erosion-controlled release; meanwhile water penetration into the matrix of the more hydrophobic 1:2 copolymer is more limited, yielding a diffusion-controlled release. *In vivo* evaluation in rabbits of 1:1 P(MAA-*co*-MMA) gels, containing salicylic acid or ketoprofen, demonstrated a

sustained release with area-under-the-curve values comparable to conventional suppositories (Witepsol[®] H-15) [52]. Drug absorption from the organogels was increased by a factor of 1.5 to 1.8 after incorporation of 10% linoleic or oleic acid, which are known permeation enhancers.

Ethanol-based organogels composed of 1:2 P(MAA-*co*-MMA) and a crosslinked poly(acrylic acid) polymer (Noveon AA-1[®]) were tested in rabbits as mucoadhesive films for immunization *via* the buccal route [86]. The antigen specific IgG titer in serum was found to be similar between rabbits having undergone buccal *versus* conventional subcutaneous immunization. Although the authors reported higher titer levels after 28 days for the buccally-immunized rabbits, the comparison seems biased given that immunization for the buccal and subcutaneous routes was achieved by different means, using plasmid-DNA encoding for the antigen *versus* the antigen itself, respectively. Nevertheless, the feasibility of buccal immunization using the novel bilayer films was successfully demonstrated.

Transnasal sustained release of propranolol hydrochloride, a β -receptor blocking agent, was obtained from biocompatible organogels consisting of SMS in isopropyl myristate, and containing small amounts of water [67]. A potential advantage of this delivery route is the circumvention of the first pass metabolism, which in the case of propranolol can reach 50-70% after oral administration. Due to water percolation and emulsification of the gel, the diffusional drug release, was found to change with time. Similarly, the SMS concentration was shown to have an optimum for achieving maximum release-

retardation. Unfortunately, even for the optimized gel formulation, the tubular network was shown to be completely disassembled within 6 h of *in vitro* exposure to water. Considerable improvements to the *in vivo* stability of these systems are needed to allow for convenient use as drug delivery systems.

5. Summary and conclusions

Given the strict requirements needed for gelation, as well as the relatively recent interest granted to organogels, many important questions still remain unanswered. For one, the precise thermodynamic and kinetic factors governing the stability of gelator fibers in the organic solvent need to be explored. Such knowledge could be applied to the systematic design of gelators yielding stable organogel systems. Furthermore, gel components could be chosen according to their compatibility with intended applications, such as non-toxic solvents for pharmaceutical formulations.

Organogels present very interesting advantages as drug delivery formulations, amongst which their ease of preparation and administration. Some organogels are currently limited by the fast diffusion of LMW drug molecules out of the matrix and/or by water infiltration into the latter. Nevertheless, optimization of sustained drug release duration is generally thought possible by fine-tuning the organogelator structure [17] and possibly the nature of the organic phase.

6. Acknowledgements

The authors wish to thank François Plourde and Nicolas Bertrand for their help in reviewing this manuscript. Funding was provided by the Canadian Institutes for Health Research (CIHR) and the Canada Research Chair program.

References

- [1] J. Lloyd, Colloid Chemistry, The Chemical Catalog Co., New York, 1926.
- [2] P. Flory, Introductory lecture, Disc Faraday Soc 57 (1974) 7.
- [3] P. Terech, R.G. Weiss, Low molecular mass gelators of organic liquids and the properties of their gels, Chem Rev 97 (1997) 3133-3159.
- [4] J.H. van Esch, B.L. Feringa, New functional materials based on self-assembling organogels: from serendipity towards design, Angew Chem Int Ed 39 (2000) 2263-2266.
- [5] S. Murdan, Organogels in drug delivery, Expert Opin Drug Deliv 2 (2005) 489-505.
- [6] A. Brizard, R. Oda, I. Huc, Chirality effects in self-assembled fibrillar networks, Top Curr Chem 256 (2005) 167-218.
- [7] J.-H. Fuhrhop, W. Helfrich, Fluid and solid fibers made of lipid molecular bilayers, Chem Rev 93 (1993) 1565-1582.
- [8] Y.A. Shchipunov, E.V. Shumilina, H. Hoffmann, Lecithin organogels with alkylglucosides, J Colloid Interface Sci 199 (1998) 218-221.
- [9] Y.A. Shchipunov, Self-organising structures of lecithin, Russian Chemical Reviews 66 (1997) 301-322.
- [10] X.Y. Liu, Gelation with small molecules: from formation mechanism to nanostructure architecture, Top Curr Chem 256 (2005) 1-37.
- [11] M. Zinic, F. Vogtle, F. Fages, Cholesterol-based gelators, Top Curr Chem 256 (2005) 39-76.
- [12] F. Fages, F. Vogtle, M. Zinic, Systematic design of amide- and urea-type gelators with tailored properties, Top Curr Chem 256 (2005) 77-131.
- [13] K. Araki, I. Yoshikawa, Nucleobase-containing gelators, Top Curr Chem 256 (2005) 133-165.
- [14] A.R. Hirst, D.K. Smith, Dendritic gelators, Top Curr Chem 256 (2005) 237-273.
- [15] O. Gronwald, S. Shinkai, Sugar-integrated gelators of organic solvents, Chemistry 7 (2001) 4328-4334.
- [16] A. Motulsky, M. Lafleur, A.C. Couffin-Hoarau, *et al.*, Characterization and biocompatibility of organogels based on L-alanine for parenteral drug delivery implants, Biomaterials 26 (2005) 6242-6253.
- [17] A.C. Couffin-Hoarau, A. Motulsky, P. Delmas, *et al.*, *In situ*-forming pharmaceutical organogels based on the self assembly of L-alanine derivatives, Pharm Res 21 (2004) 454-457.
- [18] A. Vintiloiu, M. Lafleur, G. Bastiat, *et al.*, *In situ*-forming oleogel implant for sustained release of rivastigmine, Pharm. Res. (2007) in press.
- [19] D.J. Abdallah, S.A. Sirchio, R.G. Weiss, Hexatriacontane organogels. The first determination of the conformation and molecular packing of a low-molecular-mass organogelator in its gelled state., Langmuir 16 (2000) 7558-7561.
- [20] D.J. Abdallah, R.G. Weiss, n-Alkanes gel n-alkanes (and many other organic liquids), Langmuir 16 (2000) 352-355.
- [21] K. Yoza, N. Amanokura, Y. Ono, *et al.*, Sugar-integrated gelators of organic solvents - Their remarkable diversity in gelation ability and aggregate structure, Chem Eur J 5 (1999) 2722-2729.

- [22] R. Luboradzki, O. Gronwald, A. Ikada, *et al.*, Sugar-integrated "supergelators" which can form organogels with 0.03 - 0.05 %, *Chemistry Letters* (2000) 1148-1149.
- [23] H.F. Chow, J. Zhang, C.M. Lo, *et al.*, Improving the gelation properties of 3,5-diaminobenzoate-based organogelators in aromatic solvents with additional aromatic-containing pendants, *Tetrahedron* 63 (2007) 363-373.
- [24] K. Hanabusa, Y. Maesaka, M. Kimura, *et al.*, New gelators based on 2-amino-2-phenylethanol: close gelator-chiral structure relationship, *Tetrahedron Letter* 40 (1999) 2385-2388.
- [25] U. Maitra, V.K. Potluri, N.M. Sangeetha, *et al.*, Helical aggregates from a chiral organogelator, *Tetrahedron: Assymetry* 12 (2001) 477-480.
- [26] T. Gulik-Krzywicki, C. Fouquey, J. Lehn, Electron microscopic study of supramolecular liquid crystalline polymers formed by molecular-recognition-directed self-assembly from complementary chiral components, *Proc Natl Acad Sci USA* 90 (1993) 163-167.
- [27] H. Engelkamp, S. Middelbeek, R.J. Nolte, Self-assembly of disk-shaped molecules to coiled-coil aggregates with tunable helicity, *Science* 284 (1999) 785-788.
- [28] P. Terech, V. Rodriguez, J.D. Barnes, *et al.*, Organogels and aerogels of racemic and chiral 12-hydroxyoctadecanoic acid, *Langmuir* 10 (1994) 3406-3418.
- [29] J. Jacques, A. Collet, W. S.H., *Enantiomers, racemates and resolutions*, Krieger, Malabar, 1994.
- [30] A. Vintiloiu, J.C. Leroux, unpublished data (2007).
- [31] R. Kumar, O. Katare Prakash, Lecithin organogels as a potential phospholipid-structured system for topical drug delivery: a review, *AAPS PharmSciTech* 6 (2005) E298.
- [32] R. Scartazzini, P.L. Luisi, Organogels from lecithins, *J Phys Chem* 92 (1988) 829-833.
- [33] P. Schurtenberger, R. Scartazzini, L.J. Magid, *et al.*, Structural and dynamic properties of polymer-like reverse micelles, *J Phys Chem* 94 (1990) 3695-3701.
- [34] Y.A. Shchipunov, E.V. Shumilina, Lecithin organogels: role of polar solvent and nature of intermolecular interactions, *Colloid J* 58 (1996) 117-125.
- [35] P. Schurtenberger, C. Cavaco, Polymer-like lecithin reverse micelles. 1. A light scattering study, *Langmuir* 10 (1994) 100-108.
- [36] Y.A. Shchipunov, E.V. Shumilina, Lecithin bridging by hydrogen bonds in the organogel, *Mat Sci Eng C - Biomimetic Supramol Syst* (1995) 43-50.
- [37] D. Capitani, A.L. Segre, R. Sparapani, Lecithin microemulsion gels: an NMR study of molecular mobility based on line width, *Langmuir* 7 (1991) 250-253.
- [38] D. Capitani, E. Rossi, A.L. Segre, Lecithin microemulsion gels: an NMR study, *Langmuir* 9 (1993) 685-689.
- [39] H. Willmann, P. Walde, P.L. Luisi, *et al.*, Lecithin organogel as matrix for transdermal transport of drugs, *J Pharm Sci* 81 (1992) 871-874.
- [40] D. Capitani, A.L. Segre, F. Dreher, *et al.*, Multinuclear NMR investigation of phosphatidylcholine organogels, *J Phys Chem* 100 (1996) 15211-15217.
- [41] R. Angelico, A. Ceglie, G. Colafemmina, *et al.*, Biocompatible lecithin organogels: structure and phase equilibria, *Langmuir* 21 (2005) 141-148.

- [42] Y.A. Shchipunov, Lecithin organogel: a micellar system with unique properties, *Colloid Surf A - Physicochem Eng Asp* 183-185 (2001) 541-554.
- [43] S. Murdan, G. Gregoriadis, A.T. Florence, Non-ionic surfactant based organogels incorporating niosomes, *S.T.P. Pharma Sciences* 6 (1996) 44-48.
- [44] S. Murdan, B. van den Bergh, G. Gregoriadis, *et al.*, Water-in-sorbitan monostearate organogels (water-in-oil gels), *J Pharm Sci* 88 (1999) 615-619.
- [45] S. Murdan, G. Gregoriadis, A.T. Florence, Interaction of a nonionic surfactant-based organogel with aqueous media, *Int J Pharm* 180 (1999) 211-214.
- [46] S. Murdan, G. Gregoriadis, A.T. Florence, Novel sorbitan monostearate organogels, *J Pharm Sci* 88 (1999) 608-614.
- [47] S. Murdan, G. Gregoriadis, A.T. Florence, Inverse toroidal vesicles: precursors of tubules in sorbitan monostearate organogels, *Int J Pharm* 183 (1999) 47-49.
- [48] N. Jibry, R.K. Heenan, S. Murdan, Amphiphilic gels for drug delivery: formulation and characterization, *Pharm Res* 21 (2004) 1852-1861.
- [49] R.C. Robinson, Plastibase, a hydrocarbon gel ointment base, *Bull Sch Med Univ Md* 40 (1955) 86-89.
- [50] T.A. Najjar, H.R. Sleeper, P. Calabresi, The use of 5-iodo-2'-deoxyuridine (IUDR) in Orabase and plastibase for treatment of oral herpes simplex, *J Oral Med* 24 (1969) 53-57.
- [51] A.K. Bajaj, S.C. Gupta, A.K. Chatterjee, Plastibase: a new base for patch testing of metal antigens, *Int J Dermatol* 29 (1990) 73.
- [52] S. Goto, M. Kawata, T. Suzuki, *et al.*, Preparation and evaluation of Eudragit gels. I: Eudragit organogels containing drugs as rectal sustained-release preparations, *J Pharm Sci* 80 (1991) 958-961.
- [53] M. Kawata, T. Suzuki, N.S. Kim, *et al.*, Preparation and evaluation of Eudragit gels. II: *In vitro* release of salicylic acid, sodium salicylate, and ketoprofen from Eudragit L and S organogels, *J Pharm Sci* 80 (1991) 1072-1074.
- [54] M.C. Jones, P. Tewari, C. Blei, *et al.*, Self-assembled nanocages for hydrophilic guest molecules, *J Am Chem Soc* 128 (2006) 14599-14605.
- [55] D. Grace, J. Rogers, K. Skeith, *et al.*, Topical diclofenac versus placebo: a double blind, randomized clinical trial in patients with osteoarthritis of the knee, *J Rheumatol* 26 (1999) 2659-2663.
- [56] P. Mahler, F. Mahler, H. Duruz, *et al.*, Double-blind, randomized, controlled study on the efficacy and safety of a novel diclofenac epolamine gel formulated with lecithin for the treatment of sprains, strains and contusions, *Drugs Exp Clin Res* 29 (2003) 45-52.
- [57] G. Spacca, A. Cacchio, A. Forgacs, *et al.*, Analgesic efficacy of a lecithin-vehiculated diclofenac epolamine gel in shoulder peri-arthritis and lateral epicondylitis: a placebo-controlled, multicenter, randomized, double-blind clinical trial, *Drugs Exp Clin Res* 31 (2005) 147-154.
- [58] G.P. Agrawal, M. Juneja, S. Agrawal, *et al.*, Preparation and characterization of reverse micelle based organogels of piroxicam, *Pharmazie* 59 (2004) 191-193.
- [59] C. Nastruzzi, R. Gambari, Antitumor activity of (trans)dermally delivered aromatic tetra-amidines, *J Control Release* 29 (1994) 53-62.
- [60] S. Bhatnagar, S.P. Vyas, Organogel-based system for transdermal delivery of propranolol, *J Microencapsul* 1994 (1994) 431-438.

- [61] R. Aboofazeli, H. Zia, T.E. Needham, Transdermal delivery of nicardipine: an approach to *in vitro* permeation enhancement, *Drug Deliv* 9 (2002) 239-247.
- [62] I.M. Shaikh, K.R. Jadhav, P.S. Gide, *et al.*, Topical delivery of aceclofenac from lecithin organogels: preformulation study, *Curr Drug Deliv* 3 (2006) 417-427.
- [63] F. Dreher, P. Walde, P. Walter, *et al.*, Interaction of a lecithin microemulsion gel with human stratum corneum and its effect on transdermal transport, *J Control Release* 45 (1997) 131-140.
- [64] Z.H. Gao, W.R. Crowley, A.J. Shukla, *et al.*, Controlled release of contraceptive steroids from biodegradable and injectable gel formulations - *in vivo* evaluation, *Pharm Res* 12 (1995) 864-868.
- [65] L. Kang, X.Y. Liu, P.D. Sawant, *et al.*, SMGA gels for the skin permeation of haloperidol, *J Control Release* 106 (2005) 88-98.
- [66] P.F. Lim, X.Y. Liu, L. Kang, *et al.*, Limonene GP1/PG organogel as a vehicle in transdermal delivery of haloperidol, *Int J Pharm* 311 (2006) 157-164.
- [67] S. Pisal, V. Shelke, K. Mahadik, *et al.*, Effect of organogel components on *in vitro* nasal delivery of propranolol hydrochloride, *AAPS PharmSciTech* 5 (2004) e63.
- [68] S. Murdan, T. Andrysek, D. Son, Novel gels and their dispersions - oral drug delivery systems for ciclosporin, *Int J Pharm* 300 (2005) 113-124.
- [69] S. Murdan, G. Gregoriadis, A.T. Florence, Sorbitan monostearate/polysorbate 20 organogels containing niosomes: a delivery vehicle for antigens?, *Eur J Pharm Sci* 8 (1999) 177-186.
- [70] F. Plourde, A. Motulsky, A.C. Couffin-Hoarau, *et al.*, First report on the efficacy of L-alanine-based *in situ*-forming implants for the long-term parenteral delivery of drugs, *J Control Release* 108 (2005) 433-441.
- [71] A.C. Williams, B.W. Barry, Penetration enhancers, *Adv Drug Deliv Rev* 56 (2004) 603-618.
- [72] A. Cogan, N. Garti, Microemulsions as transdermal drug delivery vehicles, *Adv Colloid Interface Sci* 123-126 (2006) 369-385.
- [73] N. Jibry, S. Murdan, *In vivo* investigation, in mice and man, into the irritation potential of novel amphiphilic gels being studied as transdermal drug carriers, *Eur J Pharm Biopharm* 58 (2004) 107-119.
- [74] M. Changez, M. Varshney, J. Chander, *et al.*, Effect of the composition of lecithin/n-propanol/isopropyl myristate/water microemulsions on barrier properties of mice skin for transdermal permeation of tetracaine hydrochloride: *in vitro*, *Colloid Surf B Biointerfaces* 50 (2006) 18-25.
- [75] A. Nokhodchi, J. Shokri, A. Dashbolaghi, *et al.*, The enhancement effect of surfactants on the penetration of lorazepam through rat skin, *Int J Pharm* 250 (2003) 359-369.
- [76] M.V.L.B. Bentley, E.R.M. Kedor, R.F. Vianna, *et al.*, The influence of lecithin and urea on the *in vitro* permeation of hydrocortisone acetate through skin from hairless mouse, *Inter J Pharm* 146 (1997) 255-262.
- [77] M. Mahjour, B. Mauser, Z. Rashidbaigi, *et al.*, Effect of egg yolk lecithins and commercial soybean lecithins on *in vitro* permeation of drugs, *J Control Release* 14 (1990) 243-252.

- [78] J.Y. Fang, T.L. Hwang, C.L. Fang, *et al.*, *In vitro* and *in vivo* evaluations of the efficacy and safety of skin permeation enhancers using flurbiprofen as a model drug, *Int J Pharm* 255 (2003) 153-166.
- [79] F. Dreher, P. Walde, P.L. Luisi, *et al.*, Human skin irritation studies of a lecithin microemulsion gel and of lecithin liposomes, *Skin Pharmacol* 9 (1996) 124-129.
- [80] T. Penzes, I. Csoka, I. Eros, Rheological analysis of the structural properties effecting the percutaneous absorption and stability in pharmaceutical organogels, *Rheol Acta* 43 (2004) 457-463.
- [81] T. Penzes, G. Blazso, Z. Aigner, *et al.*, Topical absorption of piroxicam from organogels - *in vitro* and *in vivo* correlations, *Int J Pharm* 298 (2005) 47-54.
- [82] D. Chitkara, A. Shikanov, N. Kumar, *et al.*, Biodegradable injectable *in situ* depot-forming drug delivery systems, *Macromol Biosci* 6 (2006) 977-990.
- [83] A. Hatefi, B. Amsden, Biodegradable injectable *in situ* forming drug delivery systems, *J Control Release* 80 (2002) 9-28.
- [84] L.A. Estroff, A.D. Hamilton, Water gelation by small organic molecules, *Chem Rev* 104 (2004) 1201-1218.
- [85] N.A. Peppas, P. Bures, W. Leobandung, *et al.*, Hydrogels in pharmaceutical formulations, *Eur J Pharm Biopharm* 50 (2000) 27-46.
- [86] Z. Cui, R.J. Mumper, Bilayer films for mucosal (genetic) immunization *via* the buccal route in rabbits, *Pharm Res* 19 (2002) 947-953.

CHAPTER 4

Article: *In situ*-forming oleogel implant for sustained release of rivastigmine

1. Abstract

Purpose: To provide a simplified dosing schedule and potentially reduce side effects associated to plasma peak concentrations, an *in situ*-forming oleogel implant was studied for the sustained release of rivastigmine.

Methods: The gel was prepared by dissolving 5 - 10% (w/w) N-stearoyl L-alanine methyl ester (SAM) organogelator in safflower oil containing either dissolved rivastigmine or its dispersed hydrogen tartrate salt. Rheological analysis, differential scanning calorimetry, infrared spectroscopy, and electron scanning microscopy were carried out in order to assess the impact of drug incorporation on the oleogel; this was followed by *in vitro* and *in vivo* release studies.

Results: A weakening of intermolecular interactions was suggested by gel-sol transition temperature drops of 10-15°C upon incorporation of dissolved drug. Meanwhile, the dispersed drug salt induced minimal or no changes in the transition temperature. Gels containing dispersed rivastigmine had the lowest burst *in vitro* (<15% in 24 h). *In vivo* the 10% SAM formulation containing dispersed rivastigmine provided prolonged rivastigmine release within the therapeutic range for up to 11 days, with peak plasma levels well below the toxic threshold and up to five times lower than for the control formulation.

Conclusions: This study establishes SAM gels to be a promising option for a sustained-release formulation in the treatment of Alzheimer's disease.

2. Introduction

Alzheimer's disease (AD) is the most common form of dementia amongst elderly and is estimated to afflict 18 million people worldwide [1]. Findings of the significant cholinergic deficit in AD patients [2,3] led to the common treatment involving cholinesterase inhibitors (ChEIs) that facilitate neurotransmission in remaining cholinergic neurons [4] and delay the decline of functional and cognitive ability [5]. ChEIs are presently administered orally, once to twice daily [6]. In unsupervised older adults suffering of AD, treatment compliance [7] and adherence [8,9] might be problematic, which could potentially compromise the already modest efficacy of ChEIs [10]. Adverse effects are reported to be the main reason for treatment cessation [8], and there is evidence that these can be reduced with more frequent, smaller doses [11]. These observations led to the hypothesis that a ChEI sustained release formulation would entail a possible improvement in treatment adherence and compliance, as a result of decreased side effects and simplified dosing regimens, respectively, while alleviating responsibility and workload for caregivers.

Despite the potential benefits of a sustained release of ChEIs, there have only been few and preliminary investigations to this respect. A number of studies have investigated the encapsulation of huperzine A into biodegradable microspheres of poly(*d,l*-lactic acid), PLA, and poly(*d,l*-lactide-co-glycolide), PLGA [12-14]. Huperzine A is a plant-derived ChEI that is currently approved for the treatment of AD in China. To date, sustained release formulations have been investigated for only two FDA-approved ChEIs. Release studies of tacrine from PLGA microparticles [15] showed the potential of drug delivery over prolonged periods. The major problem with tacrine is its marked hepatic toxicity,

which has limited its use in favour of the better-tolerated second-generation ChEIs (rivastigmine, donepezil, and galantamine). Out of these, rivastigmine alone has been investigated for sustained release (transdermal patch) [16].

There has been increasing interest in developing parenteral sustained-release systems for long-term drug delivery, microparticles being the most studied of such systems [17]. *In situ* forming implants, such as those composed of organogels, are also gaining in popularity due to the inherent advantages of their ease of preparation and administration [18]. Inspired by the work of Bhattacharya *et al.* who demonstrated gelation of a wide variety of organic solvents by alanine-based gelators [19], our group further investigated the thermoreversible gelation of various pharmaceutical oils by alkyl-chain derivatized L-alanine at concentrations of 10% (*w/w*) or less [20,21]. Gelling is induced by the self-assembly of gelator molecules through van der Waals interactions and hydrogen-bonding between alkyl chains and polar head-groups, respectively. The network of gelator aggregates formed immobilizes the oil and yields a semi-solid system. When injected subcutaneously to rats, the oleogel degraded over several weeks and histological analysis revealed the implants to be biocompatible [21]. A subsequent study showed the first use of these gels for the sustained release of leuprolide for 14-25 days [22]. In the present work, N-stearoyl L-alanine methyl ester (SAM) oleogels containing rivastigmine (Figure 1) were investigated as *in situ* forming implants for long-term drug-delivery, with potential use in AD treatment. The physicochemical effects of drug incorporation into the gel were studied and formulations were optimized for minimal *in vitro* burst effect. Sustained release of rivastigmine from the injectable implants was demonstrated in a pharmacokinetic study on rats.

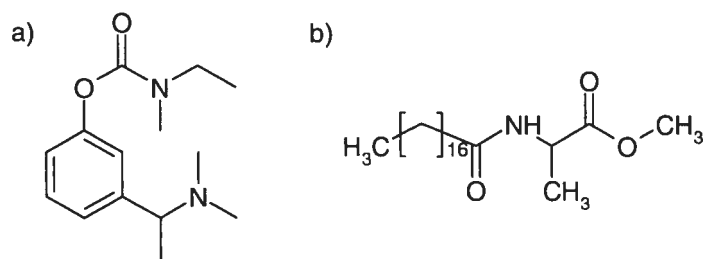


Figure 1: Molecular structures of a) rivastigmine base and b) N-stearoyl L-alanine methyl ester (SAM).

3. Materials and methods

3.1. Materials

N-methyl-2-pyrrolidone (NMP), amylamine, isopropyl alcohol, hydrogen peroxide, magnesium sulphate, sodium phosphate dibasic, trifluoroacetic acid (TFA), and sodium chloride were purchased from Sigma-Aldrich Canada Ltd. (Oakville, ON, Canada). Dichloromethane and HPLC-grade acetonitrile (ACN) were obtained from ACP (St-Leonard, QC, Canada). Sodium azide was purchased from American Chemicals Ltd. (Montreal, QC, Canada). Super Refined safflower oil and rivastigmine hydrogen tartrate (RHT) were kindly provided by Croda Inc. (Toronto, ON, Canada) and Zentiva (Prague, Czech Republic), respectively. Rivastigmine base (RB) was extracted from RHT as described below. Deionised water was generated using a Millipore Milli-Q system (Bedford, MA). SAM was synthesized as previously described [21]. RHT was tritium-labelled to a specific activity of 10 Ci/mmol by American Radiolabeled Chemicals Inc. (Saint-Louis, MO).

3.2. Preparation of Implants

Two types of gel formulations using different drug incorporation methods were investigated.

3.2.1. Dispersed-RHT Gels

For this type of formulations, the RHT powder (mean diameter (d_n) = $25 \pm 14 \mu\text{m}$, measured by light scattering in suspension on a Beckman Coulter LS230, Mississauga, Ontario, Canada) was dispersed in safflower oil at concentrations up to 5% (*w/w*). SAM organogelator was added to the oil phase in concentrations up to 10% (*w/w*). The mixture was vortexed and heated until dissolution of the organogelator. Upon cooling, the solution set to a gel containing dispersed drug particles. Unless otherwise specified, 10% (*w/w*) NMP was subsequently added to formulations, in order to decrease the gel viscosity and facilitate injection through conventional needles. After NMP addition, the gel was heated and vortexed again in order to reform a homogenous dispersion.

3.2.2. Dissolved-RB Gels

For this type of formulations, an extraction was first performed on RHT in order to isolate the RB moiety. This was done by dissolving the drug salt in deionised water and reacting it with 5 mol eq. of amylamine, thus neutralizing the base moiety and allowing the formation of an amylamine-tartrate ion pair. RB was extracted from the reaction mixture in dichloromethane, which was subsequently washed with three portions of water and dried over magnesium sulphate. The solution was filtered and the solvent evaporated to yield the RB (oily appearance). Product identity was confirmed by

¹H-NMR. The RB was directly dissolved in the safflower oil and the rest of the gel preparation was carried out as outlined above.

3.3. Characterization

3.3.1. Rheology

The rheological properties of the organogels were measured by an AR2000 (Advanced Rheometer 2000, TA Instruments, New Castle, DE), with parallel plate geometry (diameter of 40 mm). 10 % (w/w) SAM organogels in safflower oil, with 4 % (w/w) dispersed RHT or dissolved RB was heated to 80°C and the formulations were placed between the parallel plates. The final thickness of the material coat between the plates was 650 to 750 μm. The film was cooled at 4°C to form the gel. To determine the linear regime of the gel, the oscillatory strain sweeps were performed in the γ strain range from 0.003 to 50 % at 1 Hz. The linear regime is characterized by constant dynamic moduli (storage modulus, G' , and loss modulus, G'') that are independent of strain amplitude. In this regime, G' and G'' have been measured as a function of the angular frequency (0.1 to 10 Hz) at $25 \pm 0.1^\circ\text{C}$. The gel–sol (T_{GS}) transition temperature was determined by measuring G' and G'' variations at constant strain and angular frequency of 0.05 % and 1 Hz, respectively, with temperatures scanned between 25 and 80°C at 1 °C/min.

3.3.2. Differential Scanning Calorimetry (DSC)

Thermograms of dissolved-RB and dispersed-RHT gels varying in drug concentration were recorded on a 2910 TA Instruments DSC system (New Castle, DE). The calorimeter was controlled with a Thermal Solutions (Version 1.4E) interface and peak

integration was carried out using the Universal Analysis software (Version 2.5H), both from TA Instruments Inc. The instrument was calibrated with indium. Formulations were weighed into aluminum pans that were subsequently sealed. Temperature was scanned between 5 and 90°C at 10°C/min. The reported gel-sol transition temperatures (T_{GS}) corresponded to the maximum of the endothermic peaks. Six replicate analyses were conducted per formulation with one scan per sample.

3.3.3. Thermal Fourier-transform infrared (FTIR) spectroscopy

Infrared spectra of gels varying in RB concentration were recorded as a function of temperature on a Bio Rad FTS-25 spectrometer (Bio-Rad Laboratories, Randolph, MA) equipped with a water-cooled globular source, a KBr beam splitter, and a deuterated triglycine sulphate detector. The concentration of the organogelator was fixed at 10% (*w/w*) SAM and the concentration of RB dissolved in the formulation was taken to be 0, 4, and 40% (*w/w*). Once prepared, the gel was liquefied by heating and deposited between two CaF₂ windows separated by a 5- μ m Teflon spacer. This assembly was placed in a brass sample holder whose temperature was controlled by Peltier thermopumps. Starting at room temperature, the sample was heated up to 75°C in 5°-increments. At each temperature, the sample was equilibrated for 5 min before data acquisition. Each spectrum was the average of 80 scans with a nominal resolution of 2 cm⁻¹. Triplicates of each formulation were tested. Spectra were analyzed using the GRAMS software (Galactic Industry, Salem, NH).

3.3.4. Microscopy

Environmental scanning electron microscopy (ESEM) images were obtained on a Hitachi S-3000 variable pressure scanning electron microscope equipped with an environmental scanning electron detector (Hitachi, Tokyo, Japan). Accelerating voltage, operating pressure, and working distance were set to 20 kV, 120 Pa, and 9 mm, respectively. Samples studied were oleogels containing either RB, RHT, or no drug, prepared as previously described, as well as “dried gels” prepared by forming 10% SAM gels in toluene and evaporating the solvent overnight, directly on the analysis surface. Optical microscopy images of drug-free oleogels were obtained on an Axiovert S100 microscope (Carl Zeiss, Welwyn Garden City, UK) equipped with an integrated digital camera.

3.4. *In vitro* release of rivastigmine

3.4.1. Release study

Dissolved-RB and dispersed-RHT gels were prepared as described above. The organogelator concentration was varied for both types of gel up to 10% (*w/w*). NMP was added to some gels to test its effect on the release rate. The concentrations of all components in the formulation were calculated disregarding the amount of added NMP, since the solvent is expected to quickly diffuse out of the formulation upon contact with the release medium. The gels were loaded into cylindrical dialysis bags (MW cut-off 100 000 g/mol, 500 μ L) (DispoDialyzer, Fisher Scientific, Montreal, QC, Canada) using a syringe fitted with a 20-G, 1¹/₂ needle. The dialysis bag was placed in 100 mL of

phosphate-buffered saline (PBS) (104 mM NaH₂PO₄, 36 mM NaCl, 0.1% w/v NaN₃, pH 7.4) at 37°C and agitated at 135 rpm. Triplicate 1-mL samples were collected from the release medium at 15, 30 min, 1, 1.5, 2.5, 4, 6, 9, 12, 24, 48, 72 h, 7, and 14 days, with replacement of sampled volumes by fresh PBS buffer. Release kinetics were performed under sink conditions (knowing that the solubility of rivastigmine in PBS exceeds 1 mg/mL and the drug concentration in the release medium was at all times below 0.2 mg/mL). Collected samples were immediately analysed by high performance liquid chromatography (HPLC) using the method described below. Concentration values at each data point were corrected for sampling and dilution as previously described [23]. Each formulation was tested in triplicate.

3.4.2. HPLC method

In vitro release samples were analyzed using a modified liquid chromatography method previously published [24]. A Gilson Model 302 HPLC system (Gilson, Middletown, WI) equipped with a Gilson 234 autoinjector, a Gilson 106 pump, and a Gilson 151 dual-wavelength UV-detector was used. An Altima guard column (C18, 4.6 x 7.5 mm, 5 µm) (Mandel, Guelph, ON, Canada) was placed upstream of the analytical column, an XTerra (RP-18, 4.6 mm x 250 mm, 5 µm) purchased from Waters (Mississauga, ON, Canada). A mobile phase of water/ACN (78/22 v/v), containing 0.1% (v/v) TFA, was used at a flow rate of 1 mL/min. The injection volume and detection wavelength were 20 µL and 210 nm, respectively.

3.5. Pharmacokinetic study

All experimental procedures involving animals were conducted following a protocol approved by the Animal Care Committee of the University of Montreal and complied with The Guide for the Care and Use of Laboratory Animals (NIH Publication no. 85-23, revised 1996). Male Long Evans rats (200 - 225 g) (Charles River Inc. St-Constant, QC, Canada) were housed for 1 week under controlled conditions (12-h light/dark schedule, 24°C) prior to the start of experiments. Rat chow and tap water were provided *ad libitum*. All formulation components were sterilized separately. SAM was sterilized on dry ice by γ -radiation at 25 kGy using a ^{60}Co source (Nordion Inc., Laval, QC, Canada). Stability of the organogelator after sterilization was confirmed by mass spectrometry and $^1\text{H-NMR}$. The oil and NMP were filtered on 0.2- μm polytetrafluoroethylene filters. RHT was dissolved in water; the solution was spiked with the appropriate amount of ^3H -labelled drug (25 μCi /formulation) and sterilized through a 0.2- μm nylon filter. Samples were lyophilized under sterile conditions to yield a homogeneously-radiolabelled drug powder. Using the sterilized oil, SAM, NMP, and RHT, the final oil and gel formulations were prepared under aseptic conditions. A control RHT-saline solution was prepared by dissolving RHT in 0.9% NaCl solution, spiking the solution with radiolabelled drug (25 μCi /formulation) and sterilizing the final solution by filtration. The rats were divided into four groups ($n = 6$) and given a single s.c. injection of approximately 400 μL of the appropriate formulation in the lower dorsal area using a 20-G syringe. Rats were injected with the following approximate rivastigmine doses: 10 mg/kg for saline formulations and 18 mg/kg for oil and gel formulations. The exact amount of injected formulation was obtained by weight

difference of syringes before and after injection. The tested formulations were a RHT-saline solution, as well as RHT dispersed in oil, in 5%, and in 10% SAM oleogels. Blood samples (200 μL) were periodically collected from the subclavian vein of the rats under isoflurane anaesthesia, and were subsequently weighed, digested using up to 1.5 mL Solvable[®] (PerkinElmer, Groningen, The Netherlands) and 500 μL isopropyl alcohol to ensure solubility. The samples were incubated at 60°C for 1-2 h to complete digestion, after which they were bleached using 1-1.5 mL hydrogen peroxide. Finally, 10-mL portions of HionicFluor scintillation cocktail (PerkinElmer) were added to each sample, which was vortexed, stored in the dark at 4°C for 24 h, and subsequently counted on a liquid scintillation analyzer (Tricarb 2100TR, Packard, Meridan, CT). Values of drug concentration in the blood ($\mu\text{g drug/g blood}$) were obtained from the radioactivity count (dpm) of each sample by reporting the latter to the total radioactivity-to-drug ratio (dpm/ $\mu\text{g drug}$) injected.

3.6. Statistical Analysis

Tests for significant differences between means of T_{GS} , transition enthalpy (ΔH_{GS}) values, and pharmacokinetic parameters were carried out by one-way analysis of variance (ANOVA), followed where necessary by the Tukey *post-hoc* test. Differences were considered statistically significant for $p < 0.05$.

4. Results and Discussion

4.1. Physicochemical Characterization of Oleogel

4.1.1. Rheological analysis

The rheological analysis was initially performed as a function of applied strain (γ) for drug-free as well as 4 and 5% RB- or RHT-loaded oleogels, respectively, at a constant oscillation frequency of 1 Hz (Figure 2a).

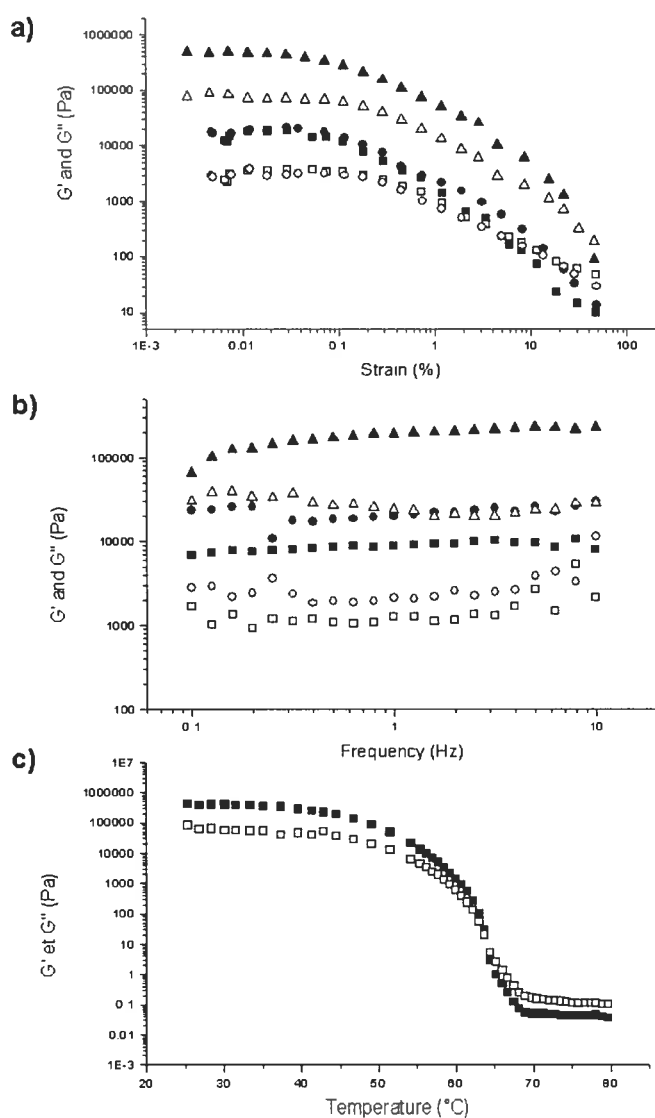


Figure 2: Rheology experiments of 10% *w/w* SAM oleogel in safflower oil containing no drug (■,□), 4% *w/w* dissolved RB (●,○), and 5% dispersed RHT (▲,△). Full and empty symbols correspond to G' and G'' , respectively. a) Strain sweep at constant frequency (1 Hz) and temperature (25°C); b) Frequency sweep at constant strain (0.01%) and temperature (25°C); c) Determination of the T_{GS} (■,□) at constant strain (0.005%) and frequency (1 Hz).

A linear regime, corresponding to strain-independent storage and loss moduli (G' and G'') was measured up to a critical strain (γ^c) value of 0.05%, beyond which a decrease in G' and G'' was observed. Using a strain value within the linear regime (0.01%), G' and G'' were measured at 25°C as a function of oscillation frequency (Table 1) and were found to be relatively constant between 0.1 and 10 Hz (Figure 2b). The G'' value of the drug free oleogel was found to be larger than 1/10 of the G' value, this being characteristic of a poorly elastic gel. Indeed, the oleogel exhibited a soft and waxy aspect. When RB was dissolved at 4% in the formulation, G' and G'' values slightly increased but remained within the same range as for the unloaded system. However, the incorporation of dispersed RHT produced a 15-fold increase of G' and G'' . These findings show that the dispersed drug improved the formulation's mechanical strength as previously observed for other gels containing physically dispersed particles [25]. Finally, the T_{GS} was determined at a strain of 0.005% and a frequency of 1 Hz (Figure 2c). At room temperature, G' was found to be higher than G'' , a property characteristic of a gel systems. As the temperature rose, G' and G'' decreased at different rates and eventually crossed, marking the system's transition to the sol-state. As shown in Table 1, RB significantly decreased the T_{GS} with respect to drug-free gels, while only a slight difference was observed for RHT-loaded formulations.

4.1.2. DSC

The effect of drug-loading on gel intermolecular interactions was evaluated based on gel-sol transitions obtained by DSC. For simplicity, only the behaviour of gels during heating cycles was investigated, however it has been previously shown that SAM oleogels undergo fully reversible transitions [21]. Analysis of oleogels containing dissolved RB (Figure 3) revealed that T_{GS} and enthalpies decreased as drug content was progressively increased from 0% (drug-free gels) to 4, 20, and 40% (*w/w*).

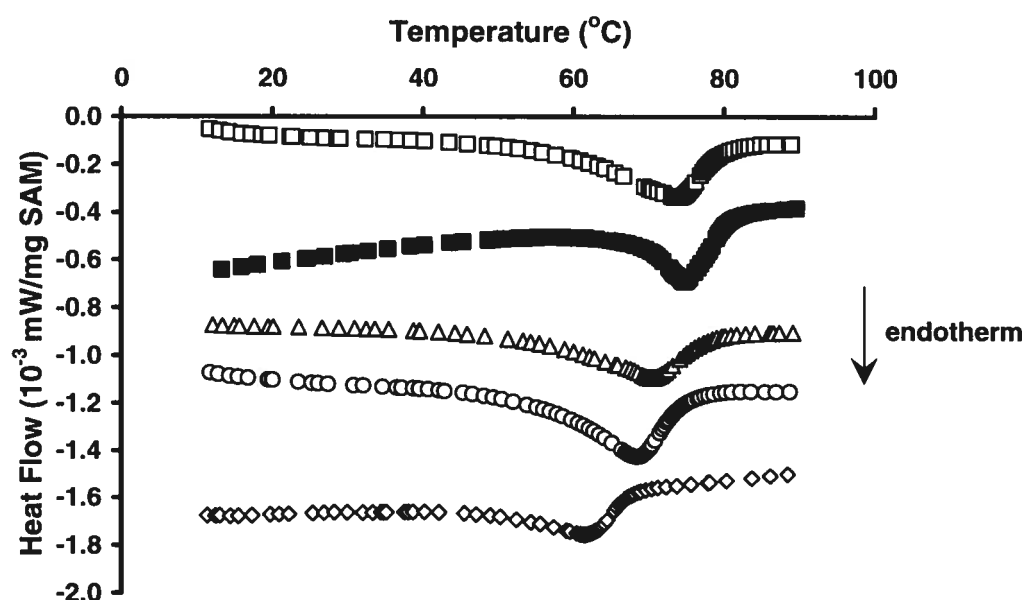


Figure 3: DSC analyses showing gel-sol transitions for drug-free gels (□), for gels containing 5% (*w/w*) dispersed RHT (■), and for gels containing RB dissolved at 4 (Δ), 20 (○), and 40% (*w/w*) (◇). Curves are offset on the y-axis for improved clarity. ΔH and T_{GS} values were calculated from the area under the curve and the temperature corresponding to the peak transition, respectively.

The drop in T_{GS} , varying between 4 and 13°C, was found to be statistically significant between any of the gels containing dissolved RB and the drug-free gel (Table 1). The DSC data corroborated well with observations from rheology measurements, both

methods indicating a decrease in T_{GS} with increasing RB-loadings. Nevertheless, T_{GS} values determined by rheological analysis were found to be 10-15°C less than those determined by DSC, an expected difference explained by the measurement of different phenomena by the two techniques. DSC further showed that transition enthalpies decreased more moderately and were found to be significantly lower than for the drug-free gel only when extremely high concentrations of RB (40% w/w) were added, yielding a 39% decrease in this case. The observation of decreasing T_{GS} and ΔH_{GS} suggests a weakening of organogelator interactions by the addition of rivastigmine. Gels containing a dispersion of RHT salt (5% w/w) were also analyzed by DSC and were found to have similar T_{GS} and ΔH_{GS} values to the drug-free formulation. This indicates that, contrary to dissolved RB, the dispersed RHT crystals do not influence the gel structure at this concentration.

Table 1. Gel characterization: 10% (w/w) SAM oleogels containing various concentrations of rivastigmine incorporated by dissolution or dispersion were characterized by rheological analysis, DSC and IR (mean \pm SD).

Drug incorporation method	Rivastigmine content % (w/w)	Rheology (n=3)		DSC (n=6)		IR (n=3)
		G'; G'' (kPa)	T_{GS} (°C)	ΔH_{GS} (J/g SAM)	T_{GS} (°C)	T_{GS} (°C)
Drug-free	0	8.29 \pm 3.65; 1.35 \pm 0.91	66.5 \pm 0.3	1.65 \pm 0.12	75.1 \pm 1.8	77.8 \pm 2.1
Dissolution	4	22.52 \pm 7.69; 1.35 \pm 0.91	54.7 \pm 0.2	1.57 \pm 0.17	70.7 \pm 1.2 ^a	75.8 \pm 4.1
	20	n.d.	n.d.	1.31 \pm 0.27	65.6 \pm 1.6 ^{a,b}	n.d.
	40	n.d.	n.d.	1.05 \pm 0.18 ^a	61.7 \pm 2.8 ^{a,b,c}	56.4 \pm 0.6 ^{a,b}
Dispersion	5	142.05 \pm 37.22 19.17 \pm 11.72	64.0 \pm 0.8	1.42 \pm 0.20 ^d	73.4 \pm 0.8 ^{c,d}	n.d.

^a $p < 0.05$ vs. drug-free gel

^b $p < 0.05$ vs. 4% (w/w) dissolved-RB gel

^c $p < 0.05$ vs. 20% (w/w) dissolved-RB gel

^d $p < 0.05$ vs. 40% (w/w) dissolved-RB gel

n.d.: not determined

4.1.3. FTIR

To gain further insight into the effect of RB addition on the gelation process, hydrogen-bonding between SAM molecules in the absence and presence of dissolved drug was studied by FTIR spectroscopy as a function of temperature (Figure 4). Two vibrational components of the amide I group were studied, indicating the presence of species identified as H-bonded (1649 cm^{-1}) and free (1685 cm^{-1}) amide carbonyl groups [21,26]. It is known that the gel-sol transition is associated with a hydrogen-bond disruption between amide groups of organogelator molecules [21,26]. This gives rise to an abrupt increase and a corresponding decrease in the peak intensities of the 1685 and 1649 cm^{-1} amide I components, respectively (Figure 5).

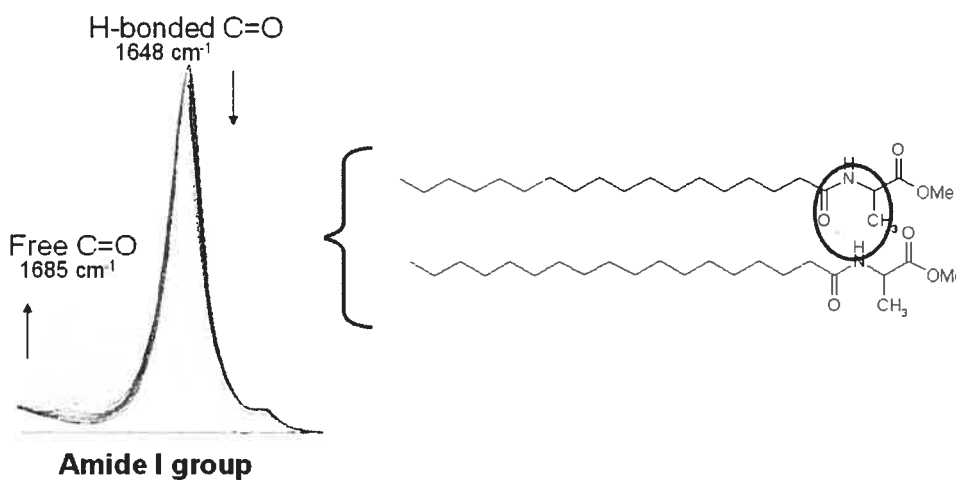


Figure 4: Thermal evolution, as probed by FTIR spectroscopy. The intensity ratio of the amide I peak components (I_{1685}/I_{1648}) was monitored as an indication of H-bond disruption between SAM molecules during gel heating from 20 to 75 °C. Arrows indicate changes from the gel (low temperatures) to the liquid (high temperatures) state.

By plotting the ratio of the peak intensity of these two bands (I_{1685}/I_{1649}) against temperature, the T_{GS} was determined from the inflection point of the corresponding sigmoidal function (Table 1).

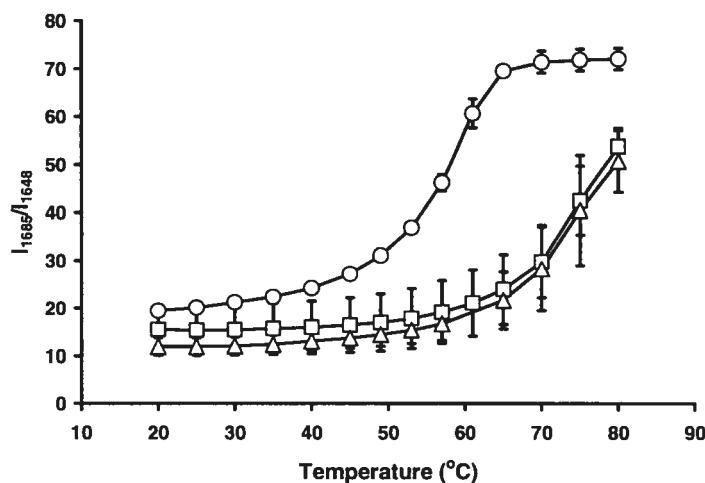


Figure 5: FTIR analysis showing the proportion of free amide bonds in drug-loaded gels, as determined from the band intensity ratio of amide I peaks at 1685 and 1648 cm^{-1} (I_{1685}/I_{1648}), as a function of temperature for gels containing dissolved RB at different concentrations: 0 (□), 4 (Δ) and 40% (*w/w*) (○) (Mean \pm SD, $n = 3$).

The T_{GS} values obtained from the IR experiment were very similar to those obtained by DSC. The drug-free and 4% (*w/w*) RB gels showed a sharp increase in the I_{1685}/I_{1649} ratio around 70°C, without the subsequent formation of a plateau, suggesting only partial network disruption for these gels at 75°C (the maximum accessible temperature for our experimental set-up). For gels with high RB concentrations (40% *w/w*), the FTIR study showed the H-bond network to be disrupted at lower temperatures ($\sim 55^\circ\text{C}$). The transition to the sol state appeared to be complete as the I_{1685}/I_{1649} ratio levelled off at around 65°C. Contrary to DSC, the IR study was not sensitive enough to show an interference of the dissolved drug with the oleogel structure at low drug-loading (4%

w/w). However, at very high drug-loading, the lowering of the transition temperature is confirmed by both the DSC and IR studies. A hypothesis for the weakening effect of the dissolved drug on the gel network is the reduction of hydrogen-bonding between organogelator amide groups by competing interactions with the ester and amine functionalities of rivastigmine. Despite this weakening effect, the formulations remain in the gel state at physiological temperature, which permits their use as drug-loaded implants.

4.1.4. Microscopy

An optical microscopy picture of drug-free, 10% SAM oleogel (Figure 6a) allowed visualisation of the continuous network of fibrous SAM aggregates responsible for gelation. Furthermore, samples of drug-free as well as RHT- and RB-loaded oleogels were analysed by ESEM (Figures 6b and c). The advantage of this technique over conventional SEM is the possibility of imaging wet and/or non-solid samples in their natural state, without sample preparation steps such as drying and metal coating. Micrographs depicted only the gel surface topography and did not allow the viewing of the underlying gelator network. Only the crests of SAM aggregates were seen protruding from the oil. The apparent aggregate size was found to be similar for drug-free gels (Figure 6b) and those containing dispersed RHT (image not shown), while being noticeably smaller in gels containing dissolved RB (Figure 6c). These observations seem to corroborate with DSC and FTIR observations, suggesting that concurrent with the hydrogen-bond disruption between SAM chains by RB, a corresponding reduction in aggregate size is possible. In a further effort to visualise the gel network, the oil was replaced with a volatile continuous phase.

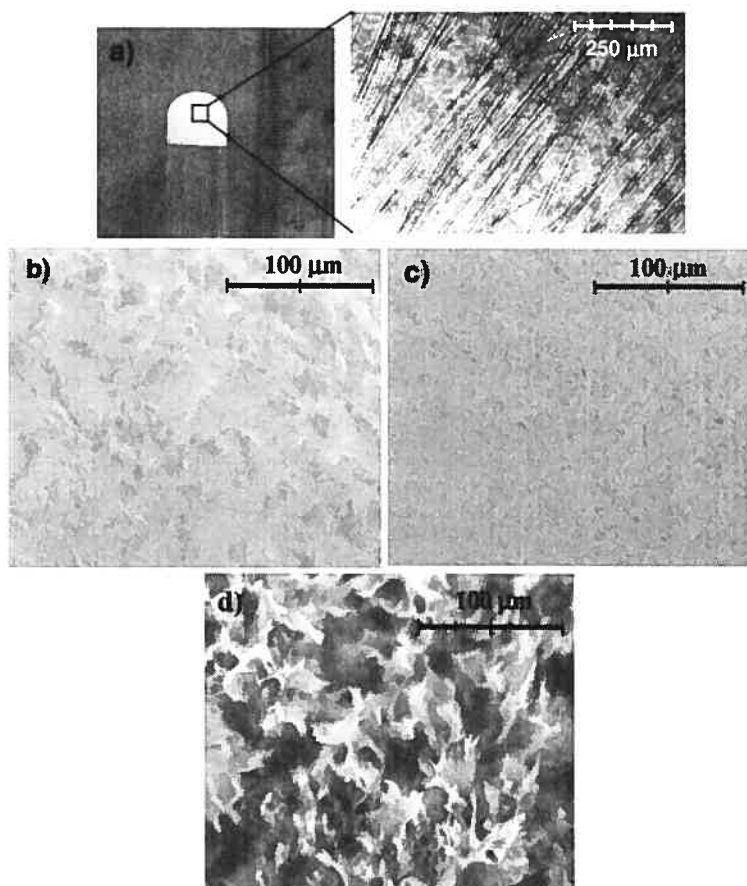


Figure 6: a) An inverted tube containing 10% (*w/w*) SAM gel is shown at room temperature to demonstrate the cohesiveness of the system. The inset shows an optical microscopy image of the oleogel network. ESEM images of a 10% (*w/w*) SAM b) drug-free oleogel and c) oleogel containing dissolved-RB (5% *w/w*). Finally, an ESEM image is shown of d) a dried formulation, obtained after complete solvent evaporation from an organogel of 10% SAM in toluene.

Although the gel structure may be different between the toluene- and oil-based formulations, gelator network formation is common to both systems. After allowing complete solvent evaporation from organogels of 10% SAM in toluene, ESEM was carried out on the dried formulations (Figure 6d). The micrograph clearly depicts the three-dimensional gelator network housing interconnected channels (dark areas) left empty by the evaporated solvent.

4.2. *In vitro* release

In vitro release kinetics were performed on oil and gel formulations (Figure 7) containing either dissolved RB (solid symbols) or dispersed RHT (hollow symbols). No true correlation of the overall release profile with eventual *in vivo* behaviour is possible given that enzymatic degradation plays a great role in the latter case. The main purpose of this study was to optimize the formulation in terms of minimal burst release, so as to diminish the risk of adverse effects *in vivo*. It is known that side-effects of rivastigmine are considerably reduced if titration of the drug is slowed down [27]. As shown in Figure 7, drug diffusion from the dialysis bag was not the rate-limiting factor, as illustrated by the complete release of drug from the control RHT solution within 6-9 h. NMP did not seem to play a significant role in the release mechanism, since formulations prepared with and without the organic solvent showed comparable burst releases (Figure 7). Its incorporation in the formulation is however beneficial because it facilitates injection at room temperature by partially disrupting the interactions between organogelator molecules [21,22].

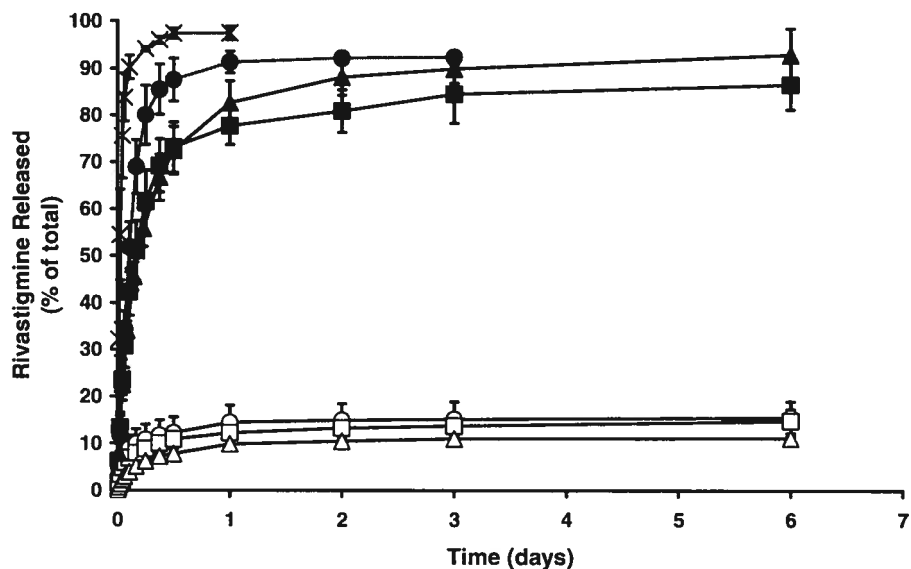


Figure 7: *In vitro* release experiments for formulations varying in SAM and NMP content as well as in drug incorporation method (dissolution vs. dispersion). A control RHT solution in PBS (X) was tested. Release experiments from formulations containing dissolved RB are represented by solid symbols: oil formulation (●), 10% SAM gel with (■) and without NMP (▲); release experiments from gels containing dispersed RHT are represented by hollow symbols: oil formulation (○) and 10% SAM gel with (□) and without NMP (△) (Mean \pm SD, n = 3).

Formulations containing dispersed RHT had a much lower burst than gels containing dissolved RB, with about 10 vs. 70-90%, respectively, of total rivastigmine released in 12 h. This is due to the limited solubility of the drug salt in the oil medium and consequently, the low amount of drug able to diffuse out of the implant. In fact, the release from these gels nearly stopped after the first day, with less than 15% of the total drug released, confirming diffusion of the drug out of the formulation to be minimal. The *in vitro* release study showed very little, if any, differences between gels varying in

organogelator concentration, especially in the case of gels containing dispersed drug. Plourde *et al.* [22] have demonstrated that the release of leuprolide from SAM oleogels varied greatly with organogelator content. The drug used in this case was incorporated into the gels via a water-in-oil emulsion, which made the density of the gel fiber network critical to the retention of emulsified water droplets. However, in the case of a simple dissolution or dispersion of the drug in the gel, the rate-limiting mechanisms of release, namely drug dissolution and/or diffusion in the oily matrix, seem to be practically unaffected by the density of the gel network, within the investigated range.

4.3. Pharmacokinetic Study

Owing to their considerably smaller burst effect, dispersed-RHT gels were chosen for subcutaneous injection to rats. Gels varying in SAM concentration (5 and 10% w/w) as well as oil and saline control formulations were studied. It is to be noted that the rivastigmine dose injected in saline (10 mg/kg) was lower than for oil and gel implants (18 mg/kg) in order to avoid overdosing, since the former formulation allows rapid systemic absorption of the entire dose. Blood concentrations of rivastigmine were monitored over two weeks. In the days following implant injection, no dermal reaction or apparent signs of toxic effects related to rivastigmine (*e.g.* diarrhea, seizures) were observed. The pharmacokinetic profiles and parameters of the injected rivastigmine formulations are presented in Figure 8 and Table 2, respectively.

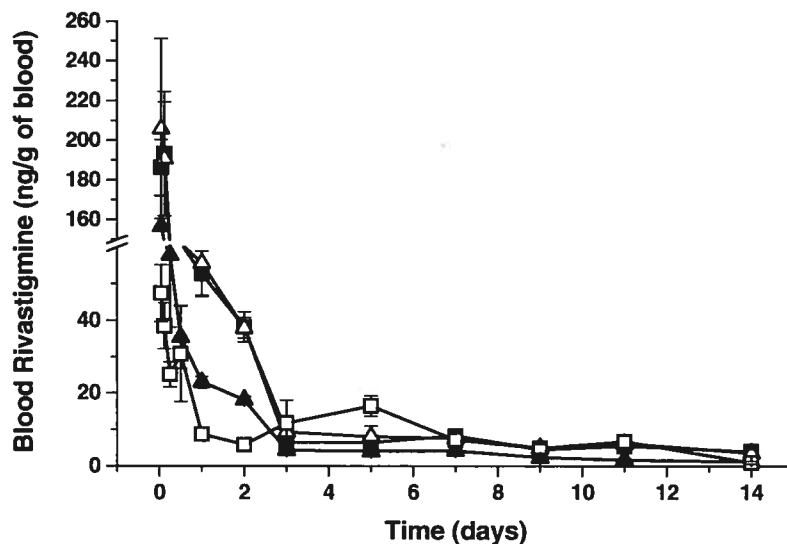


Figure 8: Blood concentration of rivastigmine after the s.c. administration of a 10 mg/kg dose of saline RHT solution (\blacktriangle), and 18 mg/kg doses of RHT dispersed in oil (\blacksquare), in 5% (\triangle), and in 10% (*w/w*) SAM gel (\square). (Mean \pm SEM, $n = 6$) SEM rather than SD values were used for the error bars in order to reduce clutter and improve the clarity.

Table 2. Pharmacokinetic parameters of the different formulations injected to rats ($n=6$).

Pharmacokinetic Parameter ^a	Formulation			
	Saline	Oil	5% SAM gel	10% SAM gel
AUC ($\text{ng}\cdot\text{day}\cdot(\text{g blood})^{-1}$)	120 \pm 20	250 \pm 62	277 \pm 101	140 \pm 70
AUC/ D_0 (10^{-4} $\text{day}\cdot(\text{g blood})^{-1}$)	6.1 \pm 1.4	8.4 \pm 2.1	7.3 \pm 4.1	4.2 \pm 2.2
C_{max} (ng/g blood)	156 \pm 37	204 \pm 73	242 \pm 102	48 \pm 17 ^{b, c}
T_{max} (min)	≤ 60	100 \pm 62	120 \pm 66	80 \pm 49

^a Values listed are the mean \pm SD.

^b $p < 0.05$ vs. oil formulation

^c $p < 0.05$ vs. 5% SAM gel formulation

Values of area under the rivastigmine blood concentration vs. time curve (AUC), obtained for days 0 to 14 by the trapezoid rule and normalized for injected dose (D_0), were not statistically different for the 4 formulations tested. This suggests a complete

release of rivastigmine from all formulations within the two weeks studied. However, despite the lack of statistical differences, a trend of decreasing AUC/D_0 can be observed with increasing organogelator concentration (8.4 vs. $4.2 \times 10^{-4} \text{ day} \cdot (\text{g blood})^{-1}$ for the oil vs. 10% SAM formulations, respectively). This observation suggests the possibility of slower, and potentially incomplete, release from the 10% SAM gels within the period studied.

As expected based on the *in vitro* experiments, the saline formulation was rapidly ($< 3 \text{ h}$) absorbed into circulation, producing an important burst, after which elimination drove drug blood levels down to baseline values within 3 days. Contrary to the *in vitro* study, there were marked differences among gels varying in SAM content. While both oil and SAM formulations showed sustained blood levels within the therapeutic range (1 – 400 ng/mL) [28] for 11 days, the 10% SAM oleogels proved largely superior to the oil and 5% SAM formulations in terms of minimizing burst release (C_{max} values up to 5 times lower). The low peak plasma concentration ($48 \pm 17 \text{ ng/g}$), being well below the toxic threshold (400 ng/mL), would allow the administration of higher rivastigmine doses, thus potentially increasing the delivery time. A hypothesis for the decrease in burst release in the case of 10% SAM formulations is the higher density of their constituting gelator network. The improved cohesiveness of these gels may reduce the subcutaneous spreading of the formulation. The potentially smaller surface area generated minimizes drug contact with the aqueous environment, contributing to a decrease in burst release.

In the time-period following the burst (days 3-7), rivastigmine plasma concentrations were maintained at higher levels in rats having received the 10% SAM implant

(7-16 ng/g blood) compared to those having received oil or 5% SAM formulations (6-9 ng/g blood). Following the burst phase, it is thought that drug release is mostly driven by implant degradation by subcutaneous esterases and lipases [29-31], a process that may be affected by gel density. The question of enzymatic degradation will be further addressed in future studies.

The only other documented pharmacokinetic study involving the sustained release of rivastigmine was conducted in minipigs and demonstrated release of the ChEI from a dermal patch for up to 72 h, with bioavailability values 20-40 times higher than for oral administration, for which the authors reported only 0.5% bioavailability [16]. Curiously enough, despite the advantages of sustained dosing regimens, no further studies were reported in the literature. The present work highlights the possibility of using L-alanine-based oleogels in the sustained release of rivastigmine for up to 11 days, demonstrating their potential use as *in situ*-forming implants for AD treatment. Future work will focus on optimizing the pharmacokinetic behaviour of these implants in the release of rivastigmine, notably by investigating release mechanisms involved and exploring the use of novel amino-acid-derived organogelators.

5. Conclusion

This study tested the sustained rivastigmine release from SAM oleogels. Physicochemical characterization contributed to the understanding of the effect of rivastigmine addition on intermolecular interactions within the gel. *In vitro* and pharmacokinetic experiments demonstrated the feasibility of using SAM oleogels for the sustained delivery of rivastigmine at therapeutic levels, and this for up to 11 days after subcutaneous injection to rats. Compared to the current once-a-day oral administration of rivastigmine, such a simplified dosing regimen has the potential to alleviate caregiver responsibilities as well as treatment-related adverse effects caused by high variations in plasma drug concentration.

6. Acknowledgements

The authors wish to thank François Plourde for his extensive help with animal studies. Funding for this project was provided by the Canadian Institutes for Health Research (CIHR).

References

- [1] C. Mount, C. Downton, Alzheimer disease: progress or profit?, *Nat Med* 12 (2006) 780-784.
- [2] R. Katzman, Alzheimer's disease, *NEJM* 314 (1986) 964-973.
- [3] C.G. Ballard, Advances in the treatment of Alzheimer's disease: benefits of dual cholinesterase inhibition, *Eur Neurol* 47 (2002) 64-70.
- [4] A. Lleo, S.M. Greenberg, J.H. Growdon, Current pharmacotherapy for Alzheimer's disease, *Ann Rev Med* 57 (2006) 513-533.
- [5] S. Gauthier, Long-term efficacy of cholinesterase inhibitors, *Brain Aging* 2 (2002) 9-22.
- [6] V.W. DeLaGarza, Pharmacologic treatment of Alzheimer's disease: an update, *Am Fam Physician* 68 (2003) 1365-1372.
- [7] V. Cotrell, K. Wild, T. Bader, Medication management and adherence among cognitively impaired older adults, *J Gerontol Soc Work* 47 (2006) 31-46.
- [8] D.G. Wilkinson, A.P. Passmore, R. Bullock, *et al.*, A mutinational, randomised, 12-week, comparative study of donepezil and rivastigmine in patients with mild to moderate Alzheimer's disease, *Int J Clin Pract* 56 (2002) 441-446.
- [9] G. Singh, S.K. Thomas, S. Arcona, *et al.*, Treatment persistency with rivastigmine and donepezil in a large state medicaid program, *J Am Geriatr Soc* 53 (2005) 1269-1270.
- [10] K.L. Lanctôt, N. Herrmann, K.K. Yau, *et al.*, Efficacy and safety of cholinesterase inhibitors in Alzheimer's disease: a meta-analysis, *Can Med Assoc J* 169 (2003) 557-564.
- [11] J. Birks, J. Grimley Evans, V. Iakovidou, *et al.*, Rivastigmine for Alzheimer's disease, *Cochrane Database Syst Rev* (2000) CD001191.
- [12] W.H. Liu, J.L. Song, K. Liu, *et al.*, Preparation and *in vitro* and *in vivo* release studies of huperzine A loaded microspheres for the treatment of Alzheimer's disease, *J Control Release* 107 (2005) 417-427.
- [13] X. Fu, Q. Ping, Y. Gao, Effects of formulation factors on encapsulation efficiency and release behaviour *in vitro* of huperzine A-PLGA microspheres, *J Microencapsul* 22 (2005) 705-714.
- [14] P. Gao, P. Ding, H. Xu, *et al.*, *In vitro* and *in vivo* characterization of huperzine A loaded microspheres made from end-group uncapped poly(d,l-lactide acid) and poly(d,l-lactide-co-glycolide acid), *Chem Pharm Bull* 54 (2006) 89-93.
- [15] Q. Yang, D. Williams, G. Owusu-Ababio, *et al.*, Controlled release tacrine delivery system for the treatment of Alzheimer's disease, *Drug Deliv* 8 (2001) 93-98.
- [16] F.L. Tse, R. Laplanche, Absorption, metabolism, and disposition of [14C]SDZ ENA 713, an acetylcholinesterase inhibitor, in minipigs following oral, intravenous, and dermal administration, *Pharm Res* 15 (1998) 1614-1620.
- [17] V.R. Sinha, A. Trehan, Biodegradable microspheres for protein delivery, *J Control Release* 90 (2003) 261-280.
- [18] C.B. Packhaeuser, J. Schnieders, C.G. Oster, *et al.*, *In situ* forming parenteral drug delivery systems: an overview, *Eur J Pharm Biopharm* 58 (2004) 445-455.

- [19] S. Bhattacharya, Y. Krishnan-Gosh, First report of phase selective gelation of oil from oil/water mixture. Possible implications toward containing oil spills., *Chem Commun* 2 (2001) 185-186.
- [20] A.C. Couffin-Hoarau, A. Motulsky, P. Delmas, *et al.*, *In situ*-forming pharmaceutical organogels based on the self assembly of L-alanine derivatives, *Pharm Res* 21 (2004) 454-457.
- [21] A. Motulsky, M. Lafleur, A.C. Couffin-Hoarau, *et al.*, Characterization and biocompatibility of organogels based on L-alanine for parenteral drug delivery implants, *Biomaterials* 26 (2005) 6242-6253.
- [22] F. Plourde, A. Motulsky, A.C. Couffin-Hoarau, *et al.*, First report on the efficacy of L-alanine-based *in situ*-forming implants for the long-term parenteral delivery of drugs, *J Control Release* 108 (2005) 433-441.
- [23] K. Fredholt, D.H. Larsen, C. Larsen, Modification of in vitro drug release rate from oily parenteral depots using a formulation approach, *Eur J Pharm Sci* 11 (2000) 231-237.
- [24] B.M. Rao, M.K. Srinivasu, K.P. Kumar, *et al.*, A stability indicating LC method for rivastigmine hydrogen tartrate, *J Pharm Biomed Anal* 37 (2005) 57-63.
- [25] S.M. Nuno-Donlucas, J.C. Sanchez-Diaz, M. Rabelero, *et al.*, Microstructured polyacrylamide hydrogels made with hydrophobic nanoparticles, *J Colloid Interface Sci* 270 (2004) 94-98.
- [26] R. Schmidt, M. Schmutz, M. Michel, *et al.*, Organogelation properties of a series of oligoamides, *Langmuir* 18 (2001) 5668-5672.
- [27] M.R. Farlow, Update on rivastigmine, *Neurolog* 9 (2003) 230-234.
- [28] Novartis, Exelon TM: Rivastigmine hydrogen tartrate, cholinesterase inhibitor, Compendium of pharmaceutical specialties (CPS), Canadian Pharmacists Association, Ottawa, 2004, pp. 835-840.
- [29] S.W. Coppack, T.J. Yost, R.M. Fisher, *et al.*, Periprandial systemic and regional lipase activity in normal humans, *Am J Physiol* 270 (1996) E718-722.
- [30] B. Jeong, Y.K. Choi, Y.H. Bae, *et al.*, New biodegradable polymers for injectable drug delivery systems, *J Control Release* 62 (1999) 109-114.
- [31] L. Appel, K. Engle, J. Jensen, *et al.*, An in vitro model to mimic in vivo subcutaneous monoolein degradation, *Pharm Res* 11 (1994) S-217.

CHAPTER 5

Results and discussion

In situ-forming SAM oleogels were prepared for the subcutaneous administration of rivastigmine, with the goal of providing a sustained release of the cholinesterase inhibitor. Gel formation is known to occur upon the self-assembly of SAM gelator molecules into fibers, stabilized by intermolecular hydrogen-bonding and van der Waals interactions [1,2]. The fibers grow to the extent of overlap and form a sample-spanning matrix that immobilizes the oil phase by surface tension. The system's physicochemical characteristics were investigated to obtain further insight into gel behaviour in response to temperature, drug-loading, and enantiomeric purity.

Texture profile analysis (Appendix 1) was conducted on drug-free oleogels to test the relationship between gelator concentration and drug strength. This technique consisted in introducing a probe into the gel sample, optimized in width and height to avoid wall-effects, and measuring the force needed for penetration to a specified depth. This experiment provided the hardness of the gel (in Newtons, N), which equals to the peak force of the first penetration. As expected from previous investigations of fatty acid-derived alanine organogels [1,2], gel strength increased with organogelator concentration (Figure 1).

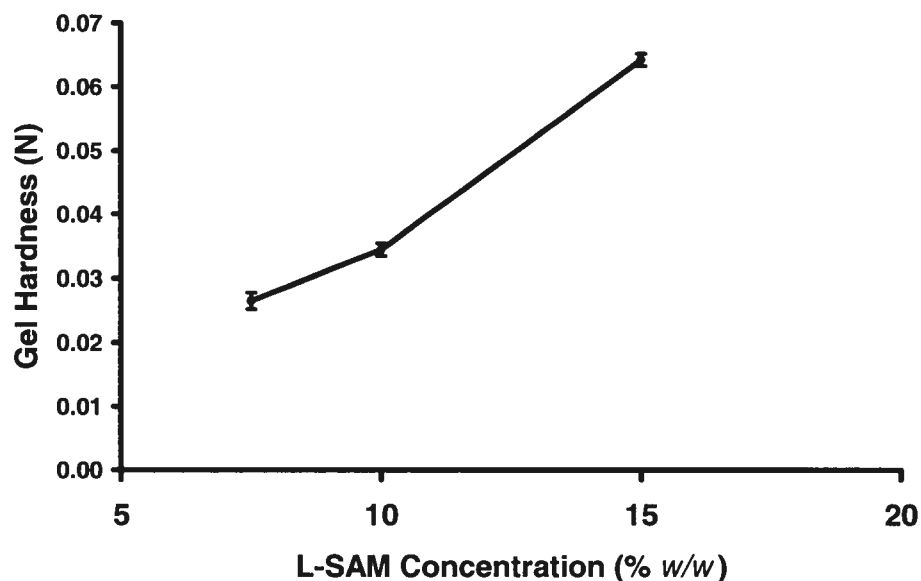
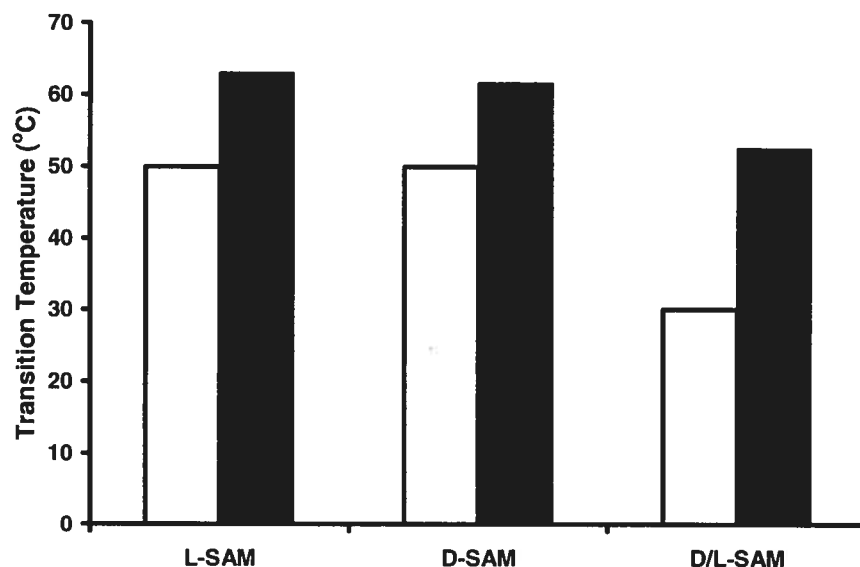


Figure 1: Average hardness of oleogels varying in SAM concentration, obtained by texture profile analysis (Mean \pm SD, $n = 3$).

These figures are lower than hardness values typically obtained for hydrogels, which generally vary between 1 [3] and 25 N [4]. However, a compromise in SAM gel hardness is needed to allow comfortable injection through conventional needles, while providing sufficient cohesiveness of the formulation once injected, to avoid excessive spreading. The *in vivo* study further highlighted the effect of varying release kinetics in terms of gelator concentration (Chapter 4, Figure 6).

As discussed in chapter 3, the presence of stereogenic centers within the gelling molecule can induce supramolecular chirality in gel fibers [5-9], therefore having a great effect on overall gel characteristics. These studies have shown chirality to have a synergistic effect on gelation; pure enantiomers often exhibit superior gelling abilities to their corresponding racemate [5]. Indeed, this general trend has been found to apply to SAM

oleogels, which exhibit significantly higher sol-gel transition temperatures when used as pure enantiomers, as opposed to a racemic mixture (Figure 2). Meanwhile, no differences in transition temperatures were detected between L- and D-SAM



oleogels.

Figure 2: Gelator chirality effect showing a decrease in DSC-determined sol-gel (white bars) and gel-sol (solid bars) transitions in racemic organogels (D/L-SAM) with respect to enantiomerically-pure L- and D-SAM. (Mean, $n = 2$).

These results have been confirmed by IR spectroscopy experiments that compared the extent of intermolecular hydrogen-bonding as a function of temperature in enantiomerically pure (L-SAM) and racemic (D/L-SAM) oleogels. Using the procedure outlined in Chapter 4, the band ratio of hydrogen-bonded (1649 cm^{-1}) and free (1685 cm^{-1}) amide carbonyl groups was plotted against temperature (Figure 3).

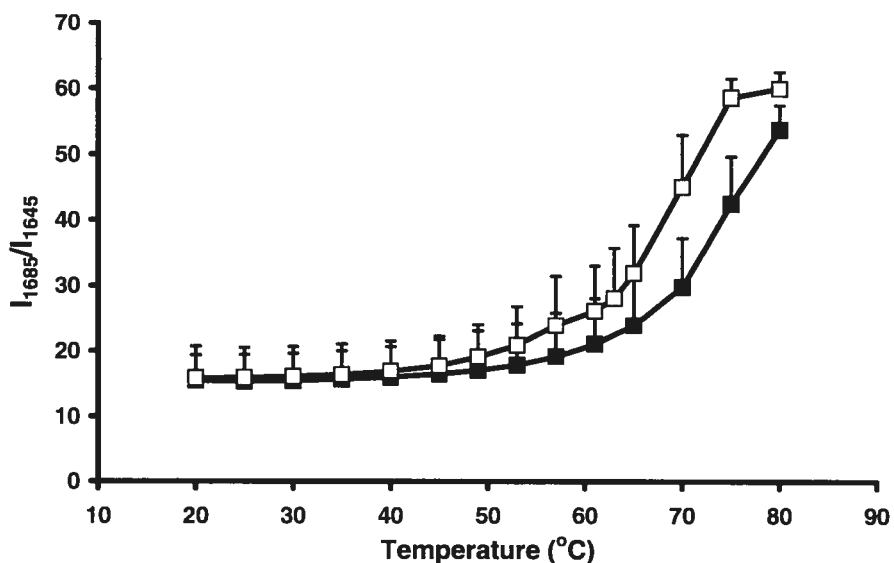


Figure 3: FTIR analysis showing the proportion of free amide bonds in drug-free gels, as determined from the band intensity ratio of amide I peaks at 1685 and 1648 cm^{-1} (I_{1685}/I_{1648}), as a function of temperature for gels prepared from 10% w/w enantiomerically pure L-SAM (■) and racemic D/L-SAM (□), respectively. (Mean \pm SD, $n = 3$)

The results obtained, indicated a slight decrease in transition temperature in the case of racemic gels, corroborating with DSC data (Figure 2). The effect of chirality was tested *in vivo*, to detect possible changes in the degradation rate of between L- and D-SAM oleogel implants, following the hypothesis that degradation of the gelator derived from the non-biological D-amino acid would be slower [10]. However, no detectable changes in remaining implant size were detected after 2- and 5-week time-points (data not shown).

Investigations were pursued using organogels prepared with L-SAM ($\geq 5\%$), in an effort to test the effect of drug loading on gel properties. DSC and FTIR results (Chapter 4, Table I) indicated a weakening of the oleogel structure by the incorporation of 4% w/w

dissolved drug, as proven by decreasing gel-sol transition temperatures. On the other hand, the dispersed RHT salt did not alter gel properties at the same concentration. Following these physicochemical investigations, *in vitro* release experiments were conducted using these oleogels to obtain information on burst release (Chapter 4, Figure 5). NMP was added to gel formulations to partially disrupt gelator interactions and to facilitate injection. Once injected, the solvent was expected to quickly diffuse out of the formulation, potentially solubilizing drug molecules on its way, thereby increasing burst release. Nevertheless, no significant difference in burst was noticed between formulations with and without NMP. When comparing the two drug incorporation methods, organogels containing dispersed rivastigmine were found to have the lowest burst (<15% in the first day). Based on these promising results, these gels were chosen for further *in vivo* investigation. The pharmacokinetic study conducted on rats demonstrated a sustained rivastigmine release within therapeutic range (1 – 400 ng/mL) for up to 11 days, with peak plasma levels well below the toxic threshold and up to five times lower than for control formulation (Chapter 4, Figure 6).

Since rivastigmine is mostly degraded by the liver, hepatic toxicity was also investigated. Histological examination of all treated and 2 untreated control rats did not reveal any significant abnormalities (data not shown). Although there was a slight degree of congestion of the sinusoids, as well as some isolated clusters of inflammatory cells, these incidental changes were minor and felt to be of no significance since they were present both in treated and control animals. Also of note, there was no evidence of bile retention, active inflammation, widening of the portal tracts or any degree of fibrosis in the

animals. This study demonstrates that no toxicity is incurred to the liver by the prolonged and sustained exposure to rivastigmine.

Overall this project succeeded in establishing SAM gels to be a promising option for a sustained-release formulation in the treatment of AD.

References

- [1] A. Motulsky, M. Lafleur, A.C. Couffin-Hoarau, *et al.*, Characterization and biocompatibility of organogels based on L-alanine for parenteral drug delivery implants, *Biomaterials* 26 (2005) 6242-6253.
- [2] A.C. Couffin-Hoarau, A. Motulsky, P. Delmas, *et al.*, *In situ*-forming pharmaceutical organogels based on the self assembly of L-alanine derivatives, *Pharm Res* 21 (2004) 454-457.
- [3] M.J. Hernandez, L. Duran, E. Costell, Influence of composition on mechanical properties of strawberry gels. Compression test and texture profile analysis, *Food Sci Tech Int* 5 (1999) 79-87.
- [4] P. Ferreira, P. Calvino, C. A.S., *et al.*, Synthesis and characterization of new methacrylate based hydrogels, *Braz J Pharm Sci* 42 (2006) 419-427.
- [5] K. Hanabusa, Y. Maesaka, M. Kimura, *et al.*, New gelators based on 2-amino-2-phenylethanol: close gelator-chiral structure relationship, *Tetrahedron Letter* 40 (1999) 2385-2388.
- [6] U. Maitra, V.K. Potluri, N.M. Sangeetha, *et al.*, Helical aggregates from a chiral organogelator, *Tetrahedron: Assymetry* 12 (2001) 477-480.
- [7] T. Gulik-Krzywicki, C. Fouquey, J. Lehn, Electron microscopic study of supramolecular liquid crystalline polymers formed by molecular-recognition-directed self-assembly from complementary chiral components, *Proc Natl Acad Sci USA* 90 (1993) 163-167.
- [8] H. Engelkamp, S. Middelbeek, R.J. Nolte, Self-assembly of disk-shaped molecules to coiled-coil aggregates with tunable helicity, *Science* 284 (1999) 785-788.
- [9] P. Terech, V. Rodriguez, J.D. Barnes, *et al.*, Organogels and aerogels of racemic and chiral 12-hydroxyoctadecanoic acid, *Langmuir* 10 (1994) 3406-3418.
- [10] N. Fujii, D-amino acid in elderly tissues, *Biol Pharm Bull* 28 (2005) 1585-1589.

CHAPTER 6

Conclusions and outlook

The eventual use of an SAM organogel as a sustained-release formulation for rivastigmine is attractive in terms of the simplified dosing schedule it would permit. This thesis outlined the investigation of the formulation's physicochemical properties as well as its *in vitro* and *in vitro* release kinetics.

It was determined that the incorporation of the dispersed RHT did not alter gel properties up to concentrations of at least 4%, while the dissolution of RB caused a decrease in gel transition temperatures at these same concentrations, as concluded from transition temperatures obtained by DSC and IR investigations. *In vitro* release profiles allowed to measure the relative burst effects of different formulations varying in SAM and NMP content, as well as in the drug incorporation method (dispersed RHT *versus* dissolved RB). The loading of oleogels with dispersed RHT permitted a substantial lowering of the burst release compared to RB-loaded oleogels (10 versus 70% of total rivastigmine released within the first 12h, respectively). Drawing on these results, a pharmacokinetic study was conducted in rats, to compare release profiles from organogels varying in SAM content and containing dispersed RHT. This experiment demonstrated the feasibility of using SAM oleogels for the sustained delivery of rivastigmine at therapeutic levels, and this for up to 11 days after subcutaneous injection. Compared to the current once-a-day oral administration of rivastigmine such a simplified dosing regimen represents an attractive alternative. Furthermore, the sustained release formulation could possibly reduce treatment-related adverse effects caused by high variations in plasma drug concentration.

The promising results obtained as part of this project warrant additional optimisation of the sustained-release duration and a further decrease in burst. This would allow the administration of higher doses while prolonging the release period. An interesting avenue currently investigated is the use of gelators using other amino acids, notably a C20-derivatized tyrosine molecule capable of gelling the oil phase at concentrations as low as 1%. Also, while the use of rivastigmine as a model drug was interesting as a proof of concept, having allowed incorporation of both hydrophilic and hydrophobic forms of the compound, the drug's efficacy in disease management is known to be modest. Consequently, future studies could focus on the incorporation of newer AD drugs with potentially better efficacy profiles. Such results would move the formulation closer to eventual usage.

APPENDIX

Methodology

Texture profile analysis

The gel samples used in the analysis were moulded in aluminum foil which was subsequently removed to avoid wall-effects. TPA analysis was conducted on a TA.XT2i texture analyzer (Texture Technologies, Hamilton, MA), using a 1 mm/s pre-test penetration speed, and a 0.1 mm/s test and post-test penetration speed. The insertion depth was set to 2 mm and the trigger force to 0.010 N.

Histology

For a histology study conducted to assess potential liver toxicity resulting from sustained exposure to rivastigmine, the whole livers of all treated and two untreated control rats were collected. Part of each organ was fixed with 10% neutral-buffered formalin. The tissue sections were processed and embedded in paraffin and glass slides with 4 μm tissue sections were prepared using a Leica 2155 microtome (Leica Microsystems Inc., Richmond Hill, ON, Canada). Slides of each liver were stained according to a hematoxylin-phloxin-safran (HPS) standard procedure [3].